

1 Spatiotemporal variations of nitrogen isotopic records 2 in the Arabian Sea

3
4 **Shuh-Ji Kao^{1*}, Baiyun Wang¹, Liwei Zheng¹, Kandasamy Selvaraj¹,**
5 **Shih-Chieh Hsu², Xianhui Sean Wan¹, Min Xu¹, Chen-Tung Arthur Chen³**

6 [1]{State Key Laboratory of Marine Environmental Science, Xiamen University,
7 Xiamen, China}

8 [2]{Research Center for Environmental Changes, Academia Sinica, Taipei, Taiwan}

9 [3]{Department of Oceanography, National Sun Yat-sen University, Kaohsiung,
10 Taiwan}

11 Correspondence to: Shuh-Ji Kao (sjkao@xmu.edu.cn)

13 **Abstract**

14 Available reports of dissolved oxygen, $\delta^{15}\text{N}$ of nitrate ($\delta^{15}\text{N}_{\text{NO}_3}$) and $\delta^{15}\text{N}$ of total
15 nitrogen ($\delta^{15}\text{N}_{\text{bulk}}$) for trap material and surface/downcore sediments from the Arabian
16 Sea (AS) were synthesized to explore its past nitrogen dynamics. Based on 25 μmol
17 kg^{-1} dissolved oxygen isopleth at 150 m deep, we classified all reported data into
18 northern and southern groups. By using $\delta^{15}\text{N}_{\text{bulk}}$ of the sediments, we obtained
19 geographically distinctive bottom-depth effects for the northern and southern AS at
20 different climate stages. After eliminating the bias caused by bottom depth, the
21 modern day sedimentary $\delta^{15}\text{N}_{\text{bulk}}$ values largely reflect the $\delta^{15}\text{N}_{\text{NO}_3}$ supply from the
22 bottom of the euphotic zone. For an addition to the dataset, nitrogen and carbon
23 contents versus their isotopic compositions of a sediment core (SK177/11) collected
24 from the most southeastern part of the AS were measured for comparison. We found a
25 one-step increase in $\delta^{15}\text{N}_{\text{bulk}}$ starting at the deglaciation with a corresponding decrease
26 in $\delta^{13}\text{C}_{\text{TOC}}$ similar to reports elsewhere revealing a global coherence. By synthesizing
27 and re-analyzing all reported down core $\delta^{15}\text{N}_{\text{bulk}}$, we derived bottom-depth correction
28 factors at different climate stages respectively for the northern and southern AS. The

1 diffusive sedimentary $\delta^{15}\text{N}_{\text{bulk}}$ values in compiled cores became confined after bias
2 correction revealing a more consistent pattern except recent 6 ka. Such high similarity
3 to the global temporal pattern indicates that the nitrogen cycle in the entire AS had
4 responded to open-ocean changes until 6 ka BP. Since 6ka BP further enhanced
5 denitrification (i.e., increase in $\delta^{15}\text{N}_{\text{bulk}}$) in the northern AS had occurred and likely
6 driven by monsoon; while in the southern we observed a synchronous reduction in
7 $\delta^{15}\text{N}_{\text{bulk}}$ implying that nitrogen fixation was promoted correspondingly as the
8 intensification of local denitrification at the northern AS basin.

9

10 **1 Introduction**

11 Biogeochemical processes of nitrogen in the ocean are intimately related to various
12 elemental cycles synergistically modulate atmospheric CO_2 and N_2O concentrations,
13 thus feedback to climate on millennial time scale (Gruber, 2004; Falkowski and
14 Godfrey, 2008; Altabet et al., 2002). Though oxygen deficient zones (ODZs) occupy
15 only ~4% of ocean volume, the denitrification process therein contributes remarkably
16 to the losses of nitrate, leaving excess P in the remaining water mass to stimulate
17 N_2 -fixation while entering euphotic zone (Morrison et al., 1998; Deutsch et al., 2007)
18 and thus controlling the budget of bio-available nitrogen in ocean. Denitrification
19 leaves $^{15}\text{NO}_3^-$ in residual nitrate (Sigman et al., 2001); whereas, N_2 -fixation
20 introduces new bio-available nitrogen with low $\delta^{15}\text{N}$ values (Capone et al., 1997) into
21 ocean for compensation. The Arabian Sea (AS), as one of the three largest ODZs in
22 the world ocean with distinctive monsoon driven upwelling, accounts for at least one
23 third of the loss of marine fixed nitrogen (Codispoti and Christensen, 1985) playing
24 an important role in the past climate via regulating atmospheric N_2O concentration
25 (Agnihotri et al., 2006) or nitrogen inventory to modulate CO_2 sequestration through
26 biological pump (Altabet, 2006).

27 Sedimentary nitrogen isotope, measured as standard δ notation with respect to
28 standards of atmospheric nitrogen, is an important tool to study the past marine
29 nitrogen cycle. Nitrogen isotope compositions of sedimentary organic matter

1 potentially reflect biological processes in water column, such as denitrification
2 (Altabet et al., 1995; Ganeshram et al., 1995, 2000), nitrogen fixation (Haug et al.,
3 1998), and the degree of nitrate utilization by algae (Altabet and Francois, 1994;
4 Holmes et al., 1996; Robinson et al., 2004). However, alteration may occur (through
5 various ways or processes, e.g., diagenesis) before the signal of $\delta^{15}\text{N}$ of exported
6 production is buried.

7 Previous measurements of $\delta^{15}\text{N}_{\text{bulk}}$ in various cores and surface sediments in the AS
8 showed the following points: 1) near-surface NO_3^- in AS is completely utilized in an
9 annual cycle, resulting in small isotopic fractionation between $\delta^{15}\text{N}$ of exported
10 sinking particles and $\delta^{15}\text{N}$ of NO_3^- supplied to the euphotic zone (Altabet, 1988;
11 Thunell et al., 2004); 2) monsoon-driven surface productivity and associated oxidant
12 demand are regarded as the main control on water column denitrification in the past
13 (Ganeshram et al., 2000; Ivanochko et al., 2005); 3) sedimentary $\delta^{15}\text{N}_{\text{bulk}}$ primarily
14 reflects the relative intensity of water column denitrification in this area (Altabet et al.,
15 1995; 1999) ; and 4) oxygen supply at intermediate depth by the Antarctic
16 Intermediate Waters (AAIW) can modulate the denitrification intensity in northern AS
17 (Schulte et al., 1999; Schmittner et al., 2007; Pichevin et al., 2007). Among previous
18 researches, the geographical features in sedimentary $\delta^{15}\text{N}_{\text{bulk}}$ between north and south
19 basins of AS have not been discussed, particularly on the basis of bottom-depth effect
20 which might be different during glacial and interglacial periods.

21 In this study, a sediment core (SK177/11) collected from the slope of southeastern AS
22 was measured for organic C and N contents and their stable isotopes. We synthesized
23 previous hydrographical and isotopic data, such as dissolved oxygen (DO), N^* ($\text{N}^* =$
24 $\text{NO}_3^- - 16 \times \text{PO}_4^{3-} + 2.9$; Gruber and Sarmiento, 2002), and $\delta^{15}\text{N}$ of nitrate as well as
25 trapped material and surface/downcore sediments, among which surface and
26 downcore sediments may have experienced more intensified diagenetic alteration.
27 Based on the subsurface DO concentration of $25 \mu\text{mol kg}^{-1}$ isopleth at 150 m, the
28 datasets in the AS were separated into north and south basins by time span (glacial,
29 Holocene and modern) for comparison. We aim to (1) investigate the geographic and

1 glacial-interglacial differences in bottom-depth effect and to (2) retrieve extra
2 information from sedimentary $\delta^{15}\text{N}_{\text{bulk}}$ by removing basin/climate stage specific
3 bottom-depth effects, thus, better decipher the environmental history of the Arabian
4 Sea.

5

6 **2 Study area**

7 The Arabian Sea is characterized by seasonal reversal of monsoon winds, resulting in
8 large seasonal physical/hydrographic/biological/chemical variations in water column
9 (Nair et al., 1989). Cold and dry northeasterly winds blow during winter from
10 high-pressure cell of the Tibetan Plateau, whereas heating of the Tibetan Plateau in
11 summer (June to September) reverses the pressure gradient leading to warm and moist
12 southwesterly winds and precipitation maximum. In present day, the SW monsoon is
13 much stronger than its northeastern counterpart.

14 The spatial distribution of DO at 150 m deep for the AS is shown in Figure 1a (World
15 Ocean Atlas 2009, <http://www.nodc.noaa.gov/OC5/WOA09/woa09data.html>), which
16 shows a clear southward increasing pattern with DO increased from ~ 5 to $>100 \mu\text{mol}$
17 kg^{-1} and the lowest DO value appears at the northeast of the northern basin. As
18 denitrification, the dominant nitrate removal process, generally occurs in the water
19 column where DO concentration ranges $0.7\sim 20 \mu\text{mol kg}^{-1}$ (Paulmier et al., 2009), the
20 intensity of denitrification was reported to descend gradually, corresponding with the
21 DO spatial pattern from northern to southern parts of AS, and became unobvious at 11
22 or 12 N (Naqvi et al., 1982). As indicated by upper 2000 m N-S transect of DO (Fig.
23 1c), a southward decreasing in ODZ thickness can be observed and the contour line of
24 $5 \mu\text{mol kg}^{-1}$ extends to around 13 N . Since the nitrate source is mainly from the
25 bottom of euphotic zone at around 150 m we postulate a geographically distinctive
26 sedimentary $\delta^{15}\text{N}_{\text{bulk}}$ underneath ODZ. Thus, an isopleth of $25 \mu\text{mol kg}^{-1}$ DO at 150 m
27 is applied as a geographic boundary to separate the northern from the southern part of
28 AS basin. The interface where DO concentration changed from 20 to $30 \mu\text{mol kg}^{-1}$
29 was such a transition zone. On the other hand, the bottom layer of ODZ moves

1 shallower toward south as shown previously by Gouretski and Koltermann (2004).
2 Accordingly, the bottom oxygen content may also be a factor to influence the degree
3 of alteration in sedimentary $\delta^{15}\text{N}_{\text{bulk}}$.

4 As mentioned in Introduction, nitrate is removed via denitrification in ODZs resulting
5 in excess P to stimulate N_2 -fixation. In Figs. 1d, 1e and 1f, we presented the N-S
6 transect of nitrate and N^* (for both the upper 2000 m and 300 m) in January. Even
7 though there contains nitrate in the very surface water (Fig. 1d), as mentioned earlier
8 near-surface NO_3^- in AS is completely utilized in an annual cycle (Altabet, 1988;
9 Thunell et al., 2004). Furthermore, negative N^* (P-excess) throughout the water
10 column represents a nitrate deficit and the lowest N^* value appears at ~300 m at
11 18-20 ‰, where DO is $<1 \mu\text{mol kg}^{-1}$. Meanwhile, a gradually southward increase in
12 N^* can be observed for upper 100 m (Fig. 1f) and the isopleth of N^* of -4 deepens
13 southward with the highest N^* (-2) appearing at ~10-12 ‰. The volume expansion of
14 high N^* water as well as a simultaneous increase in N^* strongly indicate an addition
15 of bio-available nitrogen when surface water traveling southward.

16

17 **3 Material and method**

18 A sediment gravity core, SK177/11 (8.2 ‰ and 76.47 ‰), was collected at water
19 depths of 776 m on the continental slope off southwest coast of India (Kerala) during
20 the 177th cruise of *ORV SagarKanya* on October 2002. Although the core MD77-191
21 locates further south in the AS (Bassinot et al., 2012), SK177/11 is so far the
22 southernmost core with reference to $\delta^{15}\text{N}$ record. The 3.65 m long core was
23 sub-sampled at intervals of 2 cm from top to 100 cm, and 5 cm from 100 cm to the
24 bottom of the core (open circles in Fig. 2a). There is a distinct boundary at ~1.7 m,
25 above which the core contains mainly of brownish grey clayey sediments. Neither
26 distinct laminations nor turbidities can be observed by visual contact immediately
27 after collection or at the time during sub-sampling (Pandarinath et al., 2007). All
28 sub-samples were freeze-dried and ground into powder in an agate mortar with pestle.
29 Sand was almost absent ($<1 \text{ wt.}\%$) throughout the core.

1 The calendar chronology for core SK177/11 was based on 7 accelerator mass
2 spectrometry (AMS) radiocarbon (^{14}C) dates of bulk organic matter (Fig. 2a).
3 Calendar years were calculated using calibration CALIB 6.0 with a reservoir age
4 correction of 402 years (Stuiver et al., 1998; Reimer et al., 2009). Details on the ^{14}C
5 age controlling points were presented in Table 1. Given that the AMS ^{14}C dates of
6 SK177/11 were obtained on total organic carbon, we may not be able to avoid the
7 mixture of organics of different ages during transport (Mollenhauer et al., 2005) or
8 interference by pre-aged organics sourced from land (Kao et al., 2008). However,
9 besides the reservoir age correction, higher TOC contents (Range: 2.2~5.5%) of
10 sediments and their marine-sourced organic carbon, as confirmed by stable C isotope
11 data and C/N ratio shown in Figs. 3b and 3e, we are confident that our age model is
12 reliable and less likely affected by age heterogeneity.

13 Bulk sedimentary nitrogen content and $\delta^{15}\text{N}$ analyses were carried out using a
14 Carlo-Erba EA 2100 elemental analyzer connected to a Thermo Finnigan Delta V
15 Advantage isotope ratio mass spectrometer (EA-IRMS). Sediments for total organic
16 carbon (TOC) analyses were acid-treated with 1N HCl for 16 hr, and then centrifuged
17 to remove carbonate. The acid-treated sediments were further dried at 60 °C for TOC
18 content and $\delta^{13}\text{C}$. The nitrogen isotopic compositions of acidified samples were
19 obtained in the same time for comparison. Carbon and nitrogen isotopic data were
20 presented by standard δ notation with respect to PDB carbon and atmospheric
21 nitrogen. USGS 40, which has certified $\delta^{13}\text{C}$ of -26.24‰ and $\delta^{15}\text{N}$ of -4.52‰ and
22 acetanilide (Merck) with $\delta^{13}\text{C}$ of -29.76‰ and $\delta^{15}\text{N}$ of -1.52‰ were used as working
23 standards. The reproducibility of carbon and nitrogen isotopic measurements is better
24 than 0.15‰. The precision of nitrogen and carbon content measurements were better
25 than 0.02% and 0.05%, respectively. Meanwhile, the acidified and non-acidified
26 samples exhibited identical patterns in $\delta^{15}\text{N}$ (not shown) with mean deviation of
27 0.3‰.

28

29 **4 Results**

1 **4.1 Sedimentation rate**

2 The age-depth curve was shown in Fig. 2a, in which age dates were evenly distributed
3 throughout the core though not high resolution. In Mollenhauer et al. (2005), the
4 largest age offset between total organic carbon and co-occurring foraminifera is ~3000
5 years and mostly <2000 years. Meanwhile, the offset remains more or less constant
6 throughout past 20 ka regardless of the deglacial transition. The youngest date in our
7 core is 3180 cal ka BP at 58 cm. We may expect younger age on the surface. Thus, if
8 our TOC samples contain any pre-aged organics as indicated by Mollenhaure et al.
9 (2005), the offset should not be too large to alter our interpretation for the comparison
10 between glacial and Holocene periods. The linear sedimentation rates derived from 7
11 date intervals range from 6 to 20 cm ka⁻¹ (Fig. 2b), with relatively constant value (~6
12 cm ka⁻¹) prior to Holocene except the excursion around the last glacial maximum. The
13 linear sedimentation rates started to increase since Holocene and reached 18~20 cm
14 ka⁻¹ when the sea level reached modern day level..

15 **4.2 Nitrogen and carbon contents and their isotopes**

16 Values of $\delta^{15}\text{N}_{\text{bulk}}$ ranged from 4.7‰ to 7.1‰ with significantly lower values during
17 glacial period (Fig. 3a). The $\delta^{15}\text{N}$ values increased rapidly since ~19 ka BP, with a
18 peak at ~15 ka BP and then started to decrease gradually toward modern day except
19 the low $\delta^{15}\text{N}$ excursion at ~14 ka BP. Figure 3b shows that values of $\delta^{13}\text{C}_{\text{TOC}}$
20 (-21.5~-18.5‰) were consistent with the $\delta^{13}\text{C}$ of typical marine organic matter
21 end-member (-22~-18‰; Meyers, 1997). An abrupt decrease in $\delta^{13}\text{C}$ was observed in
22 concert with the dramatic increase in $\delta^{15}\text{N}_{\text{bulk}}$ at the start of deglaciation.

23 Bulk nitrogen content (TN) had a range of 0.23~0.75% (Fig. 3c) and the total organic
24 carbon (TOC) content ranged from 2.2% to 5.5% (Fig. 3d). Both TN and TOC
25 showed similar trend over the last 35 ka BP with relatively constant values prior to
26 Holocene and an afterward elevation till modern day. The upward increasing TOC and
27 TN patterns since Holocene were consistent with the increasing pattern of
28 sedimentation rate, suggesting a higher organic burial flux induced by enhance

1 productivity, which had been reported elsewhere in the AS (Altabet et al., 2002).

2 As for TOC/TN ratio, higher values appeared during deglacial transition and glacial
3 period (Fig. 3e). The highest value coincides with the $\delta^{13}\text{C}_{\text{TOC}}$ drop implying there is
4 still some influence from terrestrial organics. However, the terrestrial organics
5 contains less nitrogen (C/N of 20; Meyers, 1997) thus the $\delta^{15}\text{N}$ did not drop
6 correspondingly. In the first meter (since ~5 ka), the downward decreasing pattern of
7 TOC and TN can also be attributed to syn-sedimentary degradation, if so a downward
8 increasing in TOC/TN should be evident. However, TOC/TN values varied in a
9 narrow range not revealing a significant increasing trend. Nevertheless, $\delta^{15}\text{N}$ and $\delta^{13}\text{C}$
10 did not show concomitant variations with C/N in the first meter or throughout the core,
11 the influence from either organic degradation or changes in terrestrial organic input on
12 isotopic signals is thus limited.

13 Figure 4 shows the scatter plot of TOC against TN. The slope of the linear regression
14 line for TOC against TN ($\text{TOC} = (6.67 \pm 0.22) \times \text{TN} + (0.99 \pm 0.11)$, $R^2 = 0.94$, $n = 57$,
15 $p < 0.0001$) is 6.67 again indicating that organic matter is mainly marine-sourced.
16 Though this slope is slightly higher than the Redfield ratio of 5.68 (wt./wt.), it is
17 lower than that observed on the East China Sea shelf (7.46; Kao et al., 2003).
18 Meanwhile, the intercept of TN is negative when TOC downs to zero implying that
19 inorganic nitrogen can be ignored in our core. Obviously, if we force the regression
20 through the origin point, TOC/TN values for samples during the Holocene will have
21 the lower ratios reflecting even less contribution from terrestrial organics.

22

23 **5 Discussion**

24 **5.1 Downward transfer and transformation of N isotopic signal**

25 As mentioned, the signal of sedimentary $\delta^{15}\text{N}$ may be altered under different burial
26 conditions. Altabet and Francois (1994) reported little diagenetic alteration of the
27 near-surface $\delta^{15}\text{N}$ in the equatorial Pacific, while apparent +5‰ enrichment relative to
28 sinking particles in the Southern Ocean, south of the polar front. In the Sargasso Sea,

1 sedimentary $\delta^{15}\text{N}$ also enriched by 3~6‰ relative to sinking particles (Altabet et al.,
2 2002; Gruber and Galloway, 2008). The degree of alteration was attributed to particle
3 sinking rate and OM preservation (Altabet, 1988). Gaye-Haake et al. (2005) also
4 suggested that low sedimentation rates benefit organic matter decomposition resulting
5 in positive shift in bulk sedimentary $\delta^{15}\text{N}$ comparing to sinking particles in South
6 China Sea. Finally, Robinson et al. (2012) concluded that oxygen exposure time at the
7 seafloor is the dominant factor controlling the extent of N isotopic alteration. Thus, it
8 is necessary to follow the track of $\delta^{15}\text{N}$ signal to clarify the occurrence of deviation
9 during transfer.

10 The reported depth profiles of $\delta^{15}\text{N}_{\text{NO}_3}$ in the AS were shown in Fig. 5, in which
11 $\delta^{15}\text{N}_{\text{NO}_3}$ values of water depth deeper than 1200 m range narrowly around 6~7‰,
12 which is slightly higher than the global average of the deep oceans ((4.8 ± 0.2)‰ for >
13 2500 m, Sigman et al., 2000; (5.7 ± 0.7)‰ for >1500 m, Liu and Kaplan, 1989).
14 Below the euphotic layer, $\delta^{15}\text{N}_{\text{NO}_3}$ increases rapidly peaking at around 200~400 m.
15 The preferential removal of $^{14}\text{NO}_3$ by water column denitrification accounts for these
16 subsurface $\delta^{15}\text{N}_{\text{NO}_3}$ highs (Brandes et al., 1998; Altabet et al., 1999; Naqvi et al.,
17 2006). The subsurface $\delta^{15}\text{N}_{\text{NO}_3}$ maximum ranges from 10 to 18‰ for different stations
18 implying a great spatial heterogeneity in water column denitrification intensity. It is
19 worth mentioning that, higher values in general appear in the northeastern AS
20 (15~18‰; Fig. 5) highlighting that the focal area of water column denitrification is
21 prone to northeastern Arabian Sea (Naqvi et al., 1994; Pichevin et al., 2007), also
22 revealed by the DO spatial distribution (Fig. 1a). Contrary to higher denitrification in
23 the northeastern AS, the export production is always higher in the northwestern AS
24 throughout a year (Rixen et al., 1996). Such decoupling between productivity and
25 denitrification was attributed to the oxygen supply by intermediate water exchange
26 besides primary productivity oxygen demand (Pichevin et al., 2007). Note that, the
27 $\delta^{15}\text{N}_{\text{NO}_3}$ values at water depth of 100~150 m, which corresponds to the bottom depth
28 of euphotic zone (Olson et al., 1993), from different stations fall within a narrow
29 range of 7~9‰ despite of wide denitrification intensity underneath. The rapid addition

1 of new nitrogen as mentioned earlier might account for the relatively uniform $\delta^{15}\text{N}_{\text{NO}_3}$
2 at the bottom of euphotic layer. Unfortunately, there no either $\delta^{15}\text{N}_{\text{NO}_3}$ profiles or
3 sediment trap data from the southern basin for comparison.

4 Interestingly, reported $\delta^{15}\text{N}$ of sinking particles ($\delta^{15}\text{N}_{\text{SP}}$) collected by five
5 sedimentation traps deployed from 500 m throughout 3200 m deep ranged narrowly
6 from 5.1~8.5‰ (Fig. 6), which is slightly lower but overlaps largely with $\delta^{15}\text{N}_{\text{NO}_3}$
7 values at 100~150 m. Such similarity in $\delta^{15}\text{N}_{\text{NO}_3}$ at 100~150 m and sinking particles
8 strongly indicated that 1) NO_3^- source for sinking particles was coming from the
9 depth around 100~150 m instead of 200~400 m, the oxygen deficient zones (ODZs)
10 where the maximum $\delta^{15}\text{N}_{\text{NO}_3}$ value occurred (Schäfer and Ittekkot, 1993; Altabet et al.,
11 1999) and 2) little alteration had occurred in $\delta^{15}\text{N}_{\text{SP}}$ along sinking in the water column
12 as indicated by Altabet (2006). There were only these five trap stations with nitrogen
13 isotope information available in the AS (Gaye-Haaake et al., 2005). The trap locations
14 were in the same area but little south comparing with $\delta^{15}\text{N}_{\text{NO}_3}$ stations (insert map in
15 Fig. 6). The slightly lower $\delta^{15}\text{N}$ in sinking particle is attributable to their geographic
16 locations (see below) since incomplete relative utilization of surface nitrate has been
17 documented to have a very limited imprint on the $\delta^{15}\text{N}$ signal in the AS (e.g., Schäfer
18 and Ittekkot, 1993).

19 The uniformly low values of $\delta^{15}\text{N}_{\text{NO}_3}$ at the bottom of euphotic zone should be a
20 consequence resulted from various processes in the euphotic zone, such as
21 remineralization, nitrification and N_2 -fixation. Nevertheless, the distribution pattern of
22 N^* (Figs. 1e and 1f) illustrates that there must be an addition of $^{14}\text{NO}_3$ into the system
23 to cancel out the isotopic enrichment caused by denitrification. Note that the positive
24 offset in $\delta^{15}\text{N}_{\text{NO}_3}$ ($\Delta\delta^{15}\text{N}_{\text{NO}_3}$, 6~12‰) in ODZs caused by various degree of
25 denitrification were narrowed down significantly while nitrate transports upward. This
26 implies that certain degree of addition processes, most likely the N_2 -fixation, varied in
27 concert with the intensity of denitrification underneath. Since the upwelling zones
28 distribute at the very north and the west of the AS and the upwelled water travels
29 southward (or outward) on the surface as shown in Fig. 1e, it is reasonable to see the

1 phenomenon of denitrification-induced N₂-fixation to compensate the nitrogen
2 deficiency. Consistent to this notion, Deutsch et al. (2007) discovered the spatial
3 coupling between denitrification in eastern tropical Pacific (upstream) and N₂-fixation
4 in western equatorial Pacific (downstream). Such horizontal nitrogen addition process
5 can also be seen clearly in our background information of N* (Fig. 1f). In fact, fixed
6 N had been proved to account for a significant part of surface nitrate in modern day
7 AS where denitrification is exceptionally intense (Brandes et al., 1998; Capone et al.,
8 1998; Parab et al., 2012).

9 Comparing with reported $\delta^{15}\text{N}$ of surface sediments retrieved from trap locations, a
10 significant positive shift in $\delta^{15}\text{N}$ can be seen at the seafloor (Fig. 6). Such positive
11 deviation can be seen elsewhere in previous reports (Altabet, 1988; Brummer et al.,
12 2002; Kienast et al., 2005) due to prolonged oxygen exposure after deposition
13 (Robinson et al., 2012) associated with sedimentation rate (Pichevin et al., 2007).
14 Although Cowie et al. (2009) found ambiguous relation between contents of
15 sedimentary organic carbon and oxygen in deep water, they also noticed the
16 appearance of maximum organic carbon contents at the lower boundary of ODZ,
17 where oxygen contents were relatively higher. Accordingly, they believed that there
18 existed other factors controlling the preservation of organic carbon, such as the
19 chemical characteristics of organic matter, the interaction between organic matters and
20 minerals, the enrichment and activity of benthic organism, or the physical factor
21 including the screening and water dynamic effect.

22 **5.2 Geographically-distinctive bottom depth effects in modern day**

23 As classified by oxygen content of 25 $\mu\text{mol kg}^{-1}$ at 150 m, documented surface
24 sedimentary $\delta^{15}\text{N}_{\text{bulk}}$ (Gaye-Haake et al., 2005) were separated into northern and
25 southern groups to examine the geographic difference in bottom-depth effect. Both
26 groups exhibit positive linear relationships between $\delta^{15}\text{N}_{\text{bulk}}$ and bottom depth (deeper
27 than 200 m) (Fig. 7a). The regression equations were shown in Table 2. Interestingly,
28 the regression differs statistically from each other in general in term of slope and

1 intercept. The slope represents the degree of positive shift of sedimentary $\delta^{15}\text{N}$ due to
2 bottom-depth effect. For the southern AS, the slope is $(0.76 \pm 0.14) \times 10^{-3} \text{ km}^{-1}$,
3 which is close to the correction factor $(0.75 \times 10^{-3} \text{ km}^{-1})$ for the world ocean proposed
4 by Robinson et al. (2012) and further applied by Galbraith et al. (2012). By contrast,
5 the slope for the northern AS is significantly lower $(0.55 \pm 0.08) \times 10^{-3} \text{ km}^{-1}$,
6 implying that the depth-associated alteration in the northern AS is smaller. The
7 correction factor for bottom-depth effect was suggested to vary in different regions
8 such as that in the South China Sea (Gaye et al., 2009). Since the magnitude of
9 oxygen exposure is the primary control of depth effect (Gaye-Haake et al., 2005;
10 Mobius et al., 2011; Robinson et al., 2012), we attributed this lower slope in the
11 northern AS to relatively higher sedimentation rates (not shown) and lower oxygen
12 contents as indicated by previous researches (Olson et al., 1993; Morrison et al., 1999;
13 Brummer et al., 2002).

14 On the other hand, the intercept for the northern AS regression (8.1 ± 0.2) is
15 significantly higher than that for the southern AS (6.0 ± 0.3) . As mentioned above,
16 $\delta^{15}\text{N}$ values of sinking particle resembled the $\delta^{15}\text{N}$ of nitrate sourced from 100~150 m
17 deep. According to the depth-dependent correction factor we may convert sedimentary
18 $\delta^{15}\text{N}_{\text{bulk}}$ values at various water depths into their initial condition when the digenic
19 alteration is minimal to represent the $\delta^{15}\text{N}$ of source nitrate. Higher intercept suggests
20 a stronger denitrification had occurred in northern AS surface sediments. The 2.1‰
21 lower intercept in the southern AS likely reflects the addition of N_2 -fixation in the
22 upper water column while it travels southward. The progressive increase of N^* toward
23 southern AS supports our speculation although none $\delta^{15}\text{N}_{\text{NO}_3}$ profiles had been
24 published in the southern basin. Future works about $\delta^{15}\text{N}_{\text{NO}_3}$ and $\delta^{15}\text{N}_{\text{SP}}$ in the
25 southern AS are needed.

26 In Fig. 7b, we presented corrected $\delta^{15}\text{N}_{\text{bulk}}$ values along with bottom depth for
27 northern and southern AS surface sediments for comparison. After removing
28 site-specific bias caused by bottom depth effect, the values and distribution ranges of
29 $\delta^{15}\text{N}_{\text{bulk}}$ for both northern and southern AS became smaller and narrower. For the

1 northern AS, the distribution pattern skewed negatively giving a standard deviation of
2 0.88‰, exactly falling in the range of 7~9‰ for $\delta^{15}\text{N}_{\text{NO}_3}$ (7~9‰) at the bottom of
3 euphotic zone. As a result, the corrected nitrogen isotopic signals in sediments more
4 truthfully represent the $\delta^{15}\text{N}_{\text{NO}_3}$ value at the bottom depth of euphotic zone.
5 Meanwhile, the statistically significant difference in $\delta^{15}\text{N}_{\text{bulk}}$ distribution between the
6 northern and southern AS further confirms the feasibility of our classification by using
7 DO isopleth of $25 \mu\text{mol kg}^{-1}$ at 150 m.

8 **5.3 Bottom-depth effect during different climate stages**

9 In order to better decipher the history of $\delta^{15}\text{N}_{\text{NO}_3}$ in the bottom euphotic zone of the
10 water column, we synthesized almost all available $\delta^{15}\text{N}_{\text{bulk}}$ of sediment cores reported
11 for the AS (see Figs. 1a and 1b for locations). Similar to modern surface sediments,
12 northern and southern groups were defined by the contour line of $25 \mu\text{mol kg}^{-1}$ DO.
13 To keep data consistency in temporal scale, we focused on the last 35 ka (Fig. 8a).
14 Unfortunately, data points were less in 0~6 ka and there were only three sediment
15 cores in southern AS, SK177/11 in this study and NIOP 905 and SO42-74KL in
16 previous studies.

17 As shown in Fig. 8a, the original $\delta^{15}\text{N}_{\text{bulk}}$ from the northern (gray dots) and southern
18 AS (green, blue and red curves) are scattering in a wide range from 4.5 to 10.5‰ over
19 entire 35 ka. The pink dots are for the data from core MD-04-2876, which is peculiar
20 since the relatively low $\delta^{15}\text{N}_{\text{bulk}}$ values deviated from all other reports in the northern
21 AS. Pichevin et al. (2007) excluded the influences from incomplete nitrate utilization
22 and terrestrial input, thus, we still include this core in our statistical analyses. As for
23 the southern cores, the temporal variations of $\delta^{15}\text{N}_{\text{bulk}}$ in core SK177/11 and NIOP 905
24 (red and blue) had a very similar trend distributing at the lower bound of whole
25 dataset. The mean $\delta^{15}\text{N}_{\text{bulk}}$ values for SK177/11 and NIOP 905 during glacial period
26 were almost identical, and the deviation in the Holocene was as small as 0.7‰. By
27 contrast, the temporal pattern for $\delta^{15}\text{N}_{\text{bulk}}$ of core SO42-74KL (green) resembles that
28 of NIOP 905 yet with an enrichment in ^{15}N by $\sim 2\text{‰}$ for the entire period. The core

1 SO42-74KL is retrieved from depth of 3212 m, which the deepest among the three
2 cores in southern AS, the positive offset is apparently caused by the bottom depth
3 effect. Thus inference should be made with caution when compare sediment cores
4 from different depths.

5 Below we consider two time spans, 0~11 ka (Holocene) and 19~35 ka (glacial), to
6 examine the bottom-depth effect at different climate stages. We ignore transgression
7 period, which is shorter with more variable in $\delta^{15}\text{N}_{\text{bulk}}$, to avoid bias caused by dating
8 uncertainties in different studies. Also, we will discuss the peculiar patters for 0~6 ka
9 later. The mean and standard deviation of reported $\delta^{15}\text{N}_{\text{bulk}}$ values for the specific time
10 span were plotted against the corresponding depth of the core. Accordingly, we
11 obtained the correction factors for glacial and early Holocene, respectively, for
12 northern and southern AS (Figs. 8b and 8c). Since only 35 ka was applied in this
13 practice, the long term alteration (Reichart et al., 1998; Altabet et al., 1999) is ignored.
14 The regression curves for modern day (dashed lines) were plotted for comparison.

15 The difference among regressions of three climate stages in northern AS (Table 2) is
16 not significant ($0.55 \times 10^{-3} \text{ km}^{-1}$ to $0.70 \times 10^{-3} \text{ km}^{-1}$); however, the regression slopes for
17 northern AS are significantly lower compared with those obtained from the southern
18 AS for all climate states. This might indicate the oxygen content in the northern AS is
19 always lower resulting in a lower degree of alteration of $\delta^{15}\text{N}_{\text{bulk}}$. On the other hand,
20 we may not exclude the effect by sedimentation rate changes over these two stages,
21 which also affect the oxygen exposure time; unfortunately, insufficient sedimentation
22 rate data in the northern AS in previous reports prevents us to implement further
23 analysis.

24 As for the southern AS, correction factors are always higher than that in northern AS.
25 The overall spatial temporal patterns are in consistent with the oxygen distribution in
26 the Arabian Sea (Olson et al., 1993; Morrison et al., 1999; Pichevin et al., 2007) and
27 agree with the view that DO concentration was the dominant factor for organic matter
28 preservation (Aller, 2001; Zonneveld et al., 2010). Meanwhile, the regression slopes
29 remained high from $0.76 \times 10^{-3} \text{ km}^{-1}$ to $1.01 \times 10^{-3} \text{ km}^{-1}$ over different climate stages in

1 the southern AS suggesting that environmental situations, thus the correction factor,
2 change less relative to that in the northern AS. For SK177/11, sedimentation rate in
3 Holocene is 2-fold higher comparing to that in glacial period; however, the influence
4 caused by sedimentation rate changes is likely not significant enough to alter the
5 regression slopes for the southern AS basing on the small changes in slope (0.93×10^{-3}
6 km^{-1} and $1.01 \times 10^{-3} \text{ km}^{-1}$).

7 **5.4 Insights from temporal changes in geographic $\delta^{15}\text{N}_{\text{bulk}}$ distribution**

8 Based on the earlier comparison among $\delta^{15}\text{N}_{\text{NO}_3}$, sinking particles and surface
9 sediments, we recognized the regression intercept is representative of the nitrogen
10 isotope of nitrate source at depth of 100 m. Therefore, the regression-derived
11 intercepts given in Table 2 can be used to infer the $\delta^{15}\text{N}_{\text{NO}_3}$ source at different climate
12 stages, while the slopes can be used as correction factors to eliminate the positive shift
13 in $\delta^{15}\text{N}_{\text{bulk}}$ caused by bottom depth; by doing this, we can get the original signal of
14 $\delta^{15}\text{N}_{\text{bulk}}$ prior to alteration. We applied the correction factor to be equal to ((bottom
15 depth – 100 m) \times slope), ignoring the sea level changes during the different climate
16 stages.

17 Noticeably, the regression intercepts for both northern and southern AS are higher in
18 the Holocene compared to that in glacial period indicating the intensified isotopic
19 enrichment in $\delta^{15}\text{N}_{\text{NO}_3}$ in entire AS in Holocene. Such increment is almost the same to
20 be $\sim 1.7\text{‰}$, which is similar to the increase in Eastern Tropical North Pacific but
21 slightly smaller than that in the Eastern Tropical South Pacific (Galbraith et al., 2012).
22 The 120 m sea level increase, which may induce only 0.1‰ offset, cannot be the
23 reason for such a significant increase of average $\delta^{15}\text{N}_{\text{bulk}}$ during the Holocene.
24 Moreover, deviations between northern and southern AS at respective climate stage
25 are almost identical (0.8‰ for Holocene and 1.0‰ for glacial) indicating a
26 synchronous shift in the relative intensity of denitrification and N_2 -fixation over the
27 basin to keep such constant latitudinal gradient of subsurface $\delta^{15}\text{N}_{\text{NO}_3}$.

28 The intermediate water formation near the polar region controls the oxygen supply to

1 the intermediate water and thus the extent of denitrification on global scale and the
2 stoichiometry of nutrient source to euphotic zone (Galbraith et al., 2004). Lower
3 glacial-stage sea surface temperature may increase oxygen solubility, while stronger
4 winds in high-latitude regions enhance the rate of thermocline ventilation. The
5 resultant colder, rapidly flushed thermocline lessened the spatial extent of
6 denitrification and, consequently, N fixation (Galbraith et al., 2004). Therefore, such a
7 basin wide synchronous increase in $\delta^{15}\text{N}_{\text{bulk}}$ is likely a global control. The lower
8 intercepts in glacial time (4.3‰ for south and 5.3‰ for north), which are similar to
9 the global mean $\delta^{15}\text{N}_{\text{NO}_3}$ (4.5~5‰, Sigman et al., 1997), illustrates a better ventilation
10 of intermediate water during glacial time in the Arabian Sea (Pichevin et al., 2007). In
11 fact, the AAIW penetrate further northward over 5°N in present day and even during
12 the late Holocene (You, 1998; Pichevin et al., 2007). Since the $\delta^{13}\text{C}$ of autochthonous
13 particulate organic carbon is negatively correlated to $[\text{CO}_2(\text{aq})]$ in euphotic zone (Rau
14 et al., 1991), the sharp decrease of $\delta^{13}\text{C}_{\text{TOC}}$ in SK177/11 at the start of deglaciation
15 (Fig. 3b) may infer the timing of a rapid accumulation of dissolved inorganic carbon
16 driven by the shrinking of oxygenated intermediate water (Pichevin et al., 2007) or
17 enhanced monsoon-driven upwelling (Ganeshram et al., 2000); both facilitate the
18 promotion of denitrification. Nevertheless, the mirror image between $\delta^{15}\text{N}$ and
19 $\delta^{13}\text{C}_{\text{TOC}}$ profiles revealed their intimate relation; of which, the variability was
20 attributable to the change of physical processes.

21 The intercepts of the northern AS increase continuously from 5.3 to 8.1 from glacial
22 through modern day indicating the strengthened intensity of denitrification relative to
23 nitrogen fixation in the northern AS (Altabet, 2007). When we take a close look at the
24 temporal pattern of corrected $\delta^{15}\text{N}_{\text{bulk}}$ for long cores (Fig. 9), we can see an amplified
25 deviation since 6 ka, during which $\delta^{15}\text{N}_{\text{bulk}}$ increases continuously in the northern AS,
26 whereas it decreases in the southern AS. (Note that the northern most core,
27 MD-04-2876, also followed the increasing trend in recent 6 ka even though its
28 $\delta^{15}\text{N}_{\text{bulk}}$ values deviated from all other cores.) Such opposite trends indicate that the
29 controlling factors on nitrogen cycle in northern AS were different from that in the

1 southern AS, which means localized enhancement in specific process had occurred.

2 Besides the oxygen supply to the intermediate water, the intensity of water column
3 denitrification varies with primary productivity (Altabet, 2006; Naqvi et al., 2006).
4 Strong summer monsoon and winter monsoon drive upwelling or convective mixing
5 to enhance the primary productivity, which in turn intensify denitrification (Altabet et
6 al., 2002; Ganeshram et al., 2002). However, it was reported also that primary
7 productivity did not correlate well with water column denitrification underneath
8 during the Holocene in some parts of the northern AS (Banakar et al., 2005 and
9 references therein). Regardless of the declining summer monsoon strength since 5500
10 ka (Hong et al., 2003), the primary productivity in northern AS seem to be increased.
11 Similar to the patterns observed for TOC and TN in this study, productivity indicators
12 (TOC and Ba/Al ratios) reported by Rao et al. (2010) in the core SK148/4 located
13 nearby our SK177/11 also increased gradually since the Holocene. Incomplete nitrate
14 consumption can hardly explain the decreasing pattern for all three cores in the
15 southern AS where upwelling intensity is much less relative to that in the north.
16 Moreover, lower TOC/TN ratios observed in Holocene in SK177/11 as mentioned
17 earlier rules out the influence from terrestrial organic input. Therefore, a spatial
18 coupling of denitrification-dependent N_2 fixation is the more plausible cause of the
19 decreasing $\delta^{15}N_{\text{bulk}}$ pattern (Deutsch et al., 2007).

20 We suggested that intensified supply of excess phosphorous (phosphorus in
21 stoichiometric excess of fixed nitrogen) toward the southern AS to stimulate N_2
22 fixation, subsequently responsible for the decreasing $\delta^{15}N_{\text{bulk}}$ pattern in the southern
23 basin. The intensification in excess phosphorous supply can be driven by enhanced
24 upwelling or intensified subsurface water column denitrification or both. According to
25 the increasing pattern in $\delta^{15}N_{\text{bulk}}$ and primary productivity in the northern AS,
26 synergetic processes are suggested. The upwelled water in northern AS basin brings
27 up low N/P water to surface for non-diazotrophs to uptake. If we assume complete
28 consumption, the remaining excess phosphorous after complete consumption will be
29 transported toward south by clockwise surface circulation and advection, therefore,

1 N₂-fixation in the southern AS acts as feedback to balance denitrification changes in
2 the northern AS. This phenomenon is similar to the illustration for the spatial coupling
3 of nitrogen inputs and losses in the Pacific Ocean proposed by Deutsch et al. (2007).
4 Why such forcing to expand the N-S deviation had not occurred before 6 ka warrants
5 more studies.

6

7 **6 Conclusions**

8 The available data showed that values of $\delta^{15}\text{N}_{\text{NO}_3}$ at the bottom of euphotic zone
9 (~150 m) were similar to $\delta^{15}\text{N}_{\text{SP}}$ implying that the source of nutrients for sinking
10 particulate organic matter was largely derived from the depth at around 150 m. Values
11 of sedimentary $\delta^{15}\text{N}_{\text{bulk}}$ were obviously higher than $\delta^{15}\text{N}_{\text{SP}}$ in surrounding areas
12 suggesting such shift of sedimentary $\delta^{15}\text{N}_{\text{bulk}}$ occurred after deposition. It is necessary
13 to remove site-specific bias of $\delta^{15}\text{N}_{\text{bulk}}$ values caused by bottom depth to retrieve the
14 original signal before alteration. As a result, the corrected nitrogen isotopic signal in
15 sediments could be representative of the value of $\delta^{15}\text{N}_{\text{NO}_3}$ at the bottom depth of
16 euphotic zone. The bottom-depth effects in the northern AS varies during different
17 climate stages, but the variation is always lower than such effect in the southern AS in
18 general. The modern surface $\delta^{15}\text{N}_{\text{bulk}}$ values can be separated statistically into northern
19 and southern AS groups reflecting a special coupling of denitrification to the north
20 and N₂-fixation to the south. This phenomenon is supported by the reported modern
21 day N* distribution. As for historical records, the offset in $\delta^{15}\text{N}_{\text{bulk}}$ between southern
22 and northern AS remained relatively constant (0.8‰ for early Holocene and 1.0‰ for
23 glacial) prior to 6 ka indicating a synchronous shift in the relative intensity of
24 denitrification and N₂-fixation over the basin to keep such constant latitudinal gradient
25 of subsurface $\delta^{15}\text{N}_{\text{NO}_3}$. However, this offset expanded gradually since 6 ka due likely
26 to more localized intensifications in denitrification and N₂-fixation had occurred,
27 respectively, in the northern and southern Arabian Seas. The spatial coupling of
28 nitrogen inputs and losses in the Arabian Sea was proposed; yet, why the driving force
29 did not expand the N-S deviation before 6 ka warrants more studies.

1

2 **Acknowledgements**

3 This research was supported by the National Natural Science Foundation of China
4 (NSFC 41176059, 91328207). KS personally thanks the Director, National Center for
5 Antarctic and Ocean Research, Goa and the Secretary, the Department of Ocean
6 Development, New Delhi, for providing the ship time, and also the crew of *ORV*
7 *Sagar Kanya* for coring operation. KS also thanks V. Yoganandan for onboard help of
8 sub-sampling and the Coordinator, Ocean Science and Technology Cell of Mangalore
9 University, for the kind encouragement.

10

11 **References**

12 Agnihotri, R., Altabet, M. A., and Herbert, T.: Influence of marine denitrification on
13 atmospheric N₂O variability during the Holocene, *Geophysical Research Letters*, 33,
14 doi:10.1029/2006GL025864, 2006.

15 Aller, R. C.: Transport and reactions in the bioirrigated zone, *The benthic boundary*
16 *layer: Transport processes and biogeochemistry*, edited by: B. Boudreau, and
17 Jørgensen, B. B., Oxford University Press, Oxford, UK, 269-301, 2001.

18 Altabet, M.: Variations in nitrogen isotopic composition between sinking and
19 suspended particles: Implications for nitrogen cycling and particle transformation in
20 the open ocean, *Deep Sea Research Part A. Oceanographic Research Papers*, 35,
21 535-554, 1988.

22 Altabet, M., and Francois, R.: Sedimentary nitrogen isotopic ratio as a recorder for
23 surface ocean nitrate utilization, *Global Biogeochemical Cycles*, 8, 103-116, 1994.

24 Altabet, M., Francois, R., Murray, D. W., and Prell, W. L.: Climate-related variations
25 in denitrification in the Arabian Sea from sediment ¹⁵N/¹⁴N ratios, *Nature*, 373,
26 506-509, 1995.

27 Altabet, M., Murray, D. W., and Prell, W. L.: Climatically linked oscillations in

1 Arabian Sea denitrification over the past 1 my: Implications for the marine N cycle,
2 *Paleoceanography*, 14, 732-743, 1999.

3 Altabet, M., Higginson, M. J., and Murray, D. W.: The effect of millennial-scale
4 changes in Arabian Sea denitrification on atmospheric CO₂, *Nature*, 415, 159-162,
5 2002.

6 Altabet, M.: Isotopic tracers of the marine nitrogen cycle: Present and past, in: *Marine*
7 *organic matter: biomarkers, isotopes and DNA*, edited by: Volkman, J. K.,
8 Springer-Verlag Berlin Heidelberg, 251-293, 2006.

9 Altabet, M.: Constraints on oceanic N balance/imbalance from sedimentary ¹⁵N
10 records, *Biogeosciences*, 4, 75-86, 2007.

11 Banakar, V., Oba, T., Chodankar, A., Kuramoto, T., Yamamoto, M., and Minagawa,
12 M.: Monsoon related changes in sea surface productivity and water column
13 denitrification in the Eastern Arabian Sea during the last glacial cycle, *Marine*
14 *Geology*, 219, 99-108, 2005.

15 Bassinot, F., Marzin, C., Braconnot, P., Marti, O., Mathien-Blard, E., Lombard, F.,
16 and Bopp, L.: Holocene evolution of summer winds and marine productivity in the
17 tropical Indian Ocean in response to insolation forcing: data-model comparison,
18 *Climate of the Past*, 7, 815-829, 2011.

19 Brandes, J. A., Devol, A. H., Yoshinari, T., Jayakumar, D., and Naqvi, S.: Isotopic
20 composition of nitrate in the central Arabian Sea and eastern tropical North Pacific: A
21 tracer for mixing and nitrogen cycles, *Limnology and Oceanography*, 43, 1680-1689,
22 1998.

23 Brummer, G., Kloosterhuis, H., and Helder, W.: Monsoon-driven export fluxes and
24 early diagenesis of particulate nitrogen and its $\delta^{15}\text{N}$ across the Somalia margin,
25 *Geological Society, London, Special Publications*, 195, 353-370, 2002.

26 Capone, D. G., Zehr, J. P., Paerl, H. W., Bergman, B., and Carpenter, E. J.:
27 *Trichodesmium*, a globally significant marine cyanobacterium, *Science*, 276,

1 1221-1229, 1997.

2 Capone, D. G., Subramaniam, A., Montoya, J. P., Voss, M., Humborg, C., Johansen,
3 A. M., Siefert, R. L., and Carpenter, E. J.: An extensive bloom of the N₂-fixing
4 cyanobacterium *Trichodesmium erythraeum* in the central Arabian Sea, *Marine*
5 *Ecology-Progress Series*, 172, 281-292, 1998.

6 Codispoti, L., and Christensen, J.: Nitrification, denitrification and nitrous oxide
7 cycling in the eastern tropical South Pacific Ocean, *Marine Chemistry*, 16, 277-300,
8 1985.

9 Cowie, G. L., Mowbray, S., Lewis, M., Matheson, H., and McKenzie, R.: Carbon and
10 nitrogen elemental and stable isotopic compositions of surficial sediments from the
11 Pakistan margin of the Arabian Sea, *Deep Sea Research Part II: Topical Studies in*
12 *Oceanography*, 56, 271-282, 2009.

13 Deutsch, C., Sarmiento, J. L., Sigman, D. M., Gruber, N., and Dunne, J. P.: Spatial
14 coupling of nitrogen inputs and losses in the ocean, *Nature*, 445, 163-167, 2007.

15 Falkowski, P. G., and Godfrey, L. V.: Electrons, life and the evolution of Earth's
16 oxygen cycle, *Philosophical Transactions of the Royal Society B: Biological Sciences*,
17 363, 2705-2716, 2008.

18 Galbraith, E. D., Kienast, M., Pedersen, T. F., and Calvert, S. E.: Glacial-interglacial
19 modulation of the marine nitrogen cycle by high-latitude O₂ supply to the global
20 thermocline, *Paleoceanography*, 19, doi:10.1029/2003PA00100, 2004.

21 Galbraith, E. D., Kienast, M., Albuquerque, A. L., Altabet, M., Batista, F., Bianchi, D.,
22 Calvert, S., Quintana, S. C., Crosta, X., Holz, R. D. P., Dubois, N., Etourneau, J.,
23 Francois, R., Hsu, T.-C., Ivanochko, T., Jaccard, S., Kao, S.-J., Kiefer, T., Kienast, S.,
24 Lehmann, M. F., Martinez, P., McCarthy, M., Meckler, A. N., Mix, A., Möbius, J.,
25 Pedersen, T., Pichevin, L., Quan, T. M., Robinson, R. S., Ryabenko, E., Schmittner,
26 A., Schneider, R., Schneider-Mor, A., Shigemitsu, M., Sinclair, D., Somes, C., Studer,
27 A., Tesdal, J. E., Thunell, R., and Yang, J.-Y.: The acceleration of oceanic
28 denitrification during deglacial warming, *Nature Geoscience*, 5, 151-156, 2012.

1 Ganeshram, R. S., Pedersen, T. F., Calvert, S. E., and Murray, J. W.: Large changes in
2 oceanic nutrient inventories from glacial to interglacial periods, *Nature*, 376, 755-758,
3 1995.

4 Ganeshram, R. S., Pedersen, T. F., Calvert, S. E., McNeill, G. W., and Fontugne, M.
5 R.: Glacial-interglacial variability in denitrification in the world's oceans: Causes and
6 consequences, *Paleoceanography*, 15, 361-376, 2000.

7 Ganeshram, R. S., Pedersen, T. F., Calvert, S., and François, R.: Reduced nitrogen
8 fixation in the glacial ocean inferred from changes in marine nitrogen and phosphorus
9 inventories, *Nature*, 415, 156-159, 2002.

10 Gaye, B., Wiesner, M., and Lahajnar, N.: Nitrogen sources in the South China Sea, as
11 discerned from stable nitrogen isotopic ratios in rivers, sinking particles, and
12 sediments, *Marine Chemistry*, 114, 72-85, 2009.

13 Gaye-Haake, B., Lahajnar, N., Emeis, K. C., Unger, D., Rixen, T., Suthhof, A.,
14 Ramaswamy, V., Schulz, H., Paropkari, A., and Guptha, M.: Stable nitrogen isotopic
15 ratios of sinking particles and sediments from the northern Indian Ocean, *Marine*
16 *Chemistry*, 96, 243-255, 2005.

17 Gouretski, V., and Koltermann, K. P.: WOCE global hydrographic climatology,
18 *Berichte des BSH*, 35, 1-52, 2004.

19 Gruber, N., and Sarmiento, J. L.: Biogeochemical/physical interactions in elemental
20 cycles, in: *The sea: Biological-Physical Interactions in the Oceans*, edited by:
21 Robinson, A. R., McCarthy, J. J., and Rothschild, B. J., John Wiley and Sons, New
22 York, 337-399, 2002.

23 Gruber, N.: The dynamics of the marine nitrogen cycle and its influence on
24 atmospheric CO₂ variations, in: *The ocean carbon cycle and climate*, edited by:
25 Follows, M., and Oguz, T., Springer Netherlands, 97-148, 2004.

26 Gruber, N., and Galloway, J. N.: An Earth-system perspective of the global nitrogen
27 cycle, *Nature*, 451, 293-296, 2008.

1 Haug, G. H., Pedersen, T. F., Sigman, D. M., Calvert, S. E., Nielsen, B., and Peterson,
2 L. C.: Glacial/interglacial variations in production and nitrogen fixation in the Cariaco
3 Basin during the last 580 kyr, *Paleoceanography*, 13, 427-432, 1998.

4 Holmes, M. E., Schneider, R. R., Müller, P. J., Segl, M., and Wefer, G.:
5 Reconstruction of past nutrient utilization in the eastern Angola Basin based on
6 sedimentary $^{15}\text{N}/^{14}\text{N}$ ratios, *Paleoceanography*, 12, 604-614, 1997.

7 Hong, Y., Hong, B., Lin, Q., Zhu, Y., Shibata, Y., Hirota, M., Uchida, M., Leng, X.,
8 Jiang, H., and Xu, H.: Correlation between Indian Ocean summer monsoon and North
9 Atlantic climate during the Holocene, *Earth and Planetary Science Letters*, 211,
10 371-380, 2003.

11 Ivanochko, T. S., Ganeshram, R. S., Brummer, G. J. A., Ganssen, G., Jung, S. J. A.,
12 Moreton, S. G., and Kroon, D.: Variations in tropical convection as an amplifier of
13 global climate change at the millennial scale, *Earth and Planetary Science Letters*, 235,
14 302-314, 2005.

15 Kao, S., Lin, F., and Liu, K.: Organic carbon and nitrogen contents and their isotopic
16 compositions in surficial sediments from the East China Sea shelf and the southern
17 Okinawa Trough, *Deep Sea Research Part II: Topical Studies in Oceanography*, 50,
18 1203-1217, 2003.

19 Kao, S., Dai, M., Wei, K., Blair, N., and Lyons, W.: Enhanced supply of fossil
20 organic carbon to the Okinawa Trough since the last deglaciation, *Paleoceanography*,
21 23, doi:10.1029/2007PA001440, 2008.

22 Kienast, M., Higginson, M., Mollenhauer, G., Eglinton, T. I., Chen, M. T., and
23 Calvert, S. E.: On the sedimentological origin of down-core variations of bulk
24 sedimentary nitrogen isotope ratios, *Paleoceanography*, 20,
25 doi:10.1029/2004PA0018081, 2005.

26 Liu, K.-K., and Kaplan, I. R.: The eastern tropical Pacific as a source of ^{15}N -enriched
27 nitrate in seawater off southern California, *Limnol. Oceanogr*, 34, 820-830, 1989.

- 1 Meyers, P. A.: Organic geochemical proxies of paleoceanographic, paleolimnologic,
2 and paleoclimatic processes, *Organic Geochemistry*, 27, 213-250, 1997.
- 3 Möbius, J., Gaye, B., Lahajnar, N., Bahlmann, E., and Emeis, K.-C.: Influence of
4 diagenesis on sedimentary $\delta^{15}\text{N}$ in the Arabian Sea over the last 130kyr, *Marine*
5 *Geology*, 284, 127-138, 2011.
- 6 Mollenhauer, G., Kienast, M., Lamy, F., Meggers, H., Schneider, R. R., Hayes, J. M.,
7 and Eglinton, T. I.: An evaluation of ^{14}C age relationships between co-occurring
8 foraminifera, alkenones, and total organic carbon in continental margin sediments,
9 *Paleoceanography*, 20, doi:10.1029/2004PA001103, 2005.
- 10 Morrison, J., Codispoti, L., Gaurin, S., Jones, B., Manghnani, V., and Zheng, Z.:
11 Seasonal variation of hydrographic and nutrient fields during the US JGOFS Arabian
12 Sea Process Study, *Deep-Sea Research Part II*, 45, 2053-2101, 1998.
- 13 Morrison, J., Codispoti, L., Smith, S. L., Wishner, K., Flagg, C., Gardner, W. D.,
14 Gaurin, S., Naqvi, S., Manghnani, V., and Prosperie, L.: The oxygen minimum zone
15 in the Arabian Sea during 1995, *Deep Sea Research Part II: Topical Studies in*
16 *Oceanography*, 46, 1903-1931, 1999.
- 17 Nair, R., Ittekkot, V., Manganini, S., Ramaswamy, V., Haake, B., Degens, E., Desai,
18 B. t., and Honjo, S.: Increased particle flux to the deep ocean related to monsoons,
19 *Nature*, 338, 749-751, 1989.
- 20 Naqvi, S., Noronha, R. J., and Reddy, C.: Denitrification in the Arabian Sea, *Deep*
21 *Sea Research Part A. Oceanographic Research Papers*, 29, 459-469, 1982.
- 22 Naqvi, S.: Denitrification processes in the Arabian Sea, *Proceedings of the Indian*
23 *Academy of Sciences-Earth and Planetary Sciences*, 103, 279-300, 1994.
- 24 Naqvi, S., Naik, H., Pratihary, A., D'Souza, W., Narvekar, P., Jayakumar, D., Devol,
25 A., Yoshinari, T., and Saino, T.: Coastal versus open-ocean denitrification in the
26 Arabian Sea, *Biogeosciences*, 3, 621-633, 2006.
- 27 Olson, D. B., Hitchcock, G. L., Fine, R. A., and Warren, B. A.: Maintenance of the

1 low-oxygen layer in the central Arabian Sea, Deep Sea Research Part II: Topical
2 Studies in Oceanography, 40, 673-685, 1993.

3 Pandarinath, K., Subrahmanya, K., Yadava, M., and Verma, S.: Late Quaternary
4 Sedimentation Records on the Continental Slope Off Southwest Coast of
5 India-Implications for Provenance, Depositional and Paleomonsoonal Conditions,
6 Journal of the Geological Society of India, 69, 1285-1292, 2007.

7 Parab, S. G., and Matondkar, S.: Primary productivity and nitrogen fixation by
8 *Trichodesmium spp.* in the Arabian Sea, Journal of Marine Systems, 105, 82-95, 2012.

9 Paulmier, A., and Ruiz-Pino, D.: Oxygen minimum zones (OMZs) in the modern
10 ocean, Progress in Oceanography, 80, 113-128, 2009.

11 Pichevin, L., Bard, E., Martinez, P., and Billy, I.: Evidence of ventilation changes in
12 the Arabian Sea during the late Quaternary: Implication for denitrification and nitrous
13 oxide emission, Global Biogeochemical Cycles, 21, doi:10.1029/2006GB002852,
14 2007.

15 Rao, V. P., Kessarkar, P. M., Thamban, M., and Patil, S. K.: Paleoclimatic and
16 diagenetic history of the late quaternary sediments in a core from the Southeastern
17 Arabian Sea: Geochemical and magnetic signals, Journal of oceanography, 66,
18 133-146, 2010.

19 Rau, G., Froelich, P. N., Takahashi, T., and Des Marais, D.: Does sedimentary organic
20 $\delta^{13}\text{C}$ record variations in Quaternary ocean $[\text{CO}_2(\text{aq})]$, Paleoceanography, 6, 335-347,
21 1991.

22 Reichart, G.-J., Lourens, L., and Zachariasse, W.: Temporal variability in the northern
23 Arabian Sea Oxygen Minimum Zone (OMZ) during the last 225,000 years,
24 Paleoceanography, 13, 607-621, 1998.

25 Reimer, P. J., Baillie, M. G., Bard, E., Bayliss, A., Beck, J. W., Blackwell, P. G.,
26 Ramsey, C. B., Buck, C. E., Burr, G. S., and Edwards, R. L.: IntCal09 and Marine09
27 radiocarbon age calibration curves, 0-50,000 yeats cal BP, Radiocarbon, 51,

1 1111-1150, 2009.

2 Rixen, T., Haake, B., Ittekkot, V., Guptha, M., Nair, R., and Schlüssel, P.: Coupling
3 between SW monsoon-related surface and deep ocean processes as discerned from
4 continuous particle flux measurements and correlated satellite data, *Journal of*
5 *geophysical research*, 101, 28569-28528, 1996.

6 Robinson, R. S., Brunelle, B. G., and Sigman, D. M.: Revisiting nutrient utilization in
7 the glacial Antarctic: Evidence from a new method for diatom-bound N isotopic
8 analysis, *Paleoceanography*, 19, doi:10.1029/2003PA000996, 2004.

9 Robinson, R. S., Kienast, M., Luiza Albuquerque, A., Altabet, M., Contreras, S., De
10 Pol Holz, R., Dubois, N., Francois, R., Galbraith, E., and Hsu, T. C.: A review of
11 nitrogen isotopic alteration in marine sediments, *Paleoceanography*, 27,
12 doi:10.1029/2012PA002321, 2012.

13 Schäfer, P., and Ittekkot, V.: Seasonal variability of $\delta^{15}\text{N}$ in settling particles in the
14 Arabian Sea and its palaeogeochemical significance, *Naturwissenschaften*, 80,
15 511-513, 1993.

16 Schmittner, A., Galbraith, E. D., Hostetler, S. W., Pedersen, T. F., and Zhang, R.:
17 Large fluctuations of dissolved oxygen in the India and Pacific oceans during
18 Dansgaard-Oeschger oscillations caused by variations of North Atlantic Deep Water
19 subduction, *Paleoceanography*, 22, doi:10.1029/2006PA001384, 2007.

20 Schubert, C. J., and Calvert, S. E.: Nitrogen and carbon isotopic composition of
21 marine and terrestrial organic matter in Arctic Ocean sediments: implications for
22 nutrient utilization and organic matter composition, *Deep Sea Research Part I:*
23 *Oceanographic Research Papers*, 48, 789-810, 2001.

24 Schulte, S., Rostek, F., Bard, E., Rullkötter, J., and Marchal, O.: Variations of
25 oxygen-minimum and primary productivity recorded in sediments of the Arabian Sea,
26 *Earth and Planetary Science Letters*, 173, 205-221, 1999.

27 Sigman, D., Altabet, M., Michener, R., McCorkle, D., Fry, B., and Holmes, R.:

1 Natural abundance-level measurement of the nitrogen isotopic composition of oceanic
2 nitrate: an adaptation of the ammonia diffusion method, *Marine Chemistry*, 57,
3 227-242, 1997.

4 Sigman, D., Altabet, M., McCorkle, D., Francois, R., and Fischer, G.: The $\delta^{15}\text{N}$ of
5 nitrate in the Southern Ocean: nitrogen cycling and circulation in the ocean interior,
6 *Journal of Geophysical Research: Oceans* (1978–2012), 105, 19599-19614, 2000.

7 Sigman, D. M., Karsh, K. L., and Casciotti, K. L.: Nitrogen Isotopes in the Ocean, in:
8 *Encyclopedia of Ocean Sciences*, edited by: John, H. S. (Editor-in-Chief), Academic
9 Press, Oxford, 1884-1894, 2001.

10 Stuiver, M., and Braziunas, T. F.: Anthropogenic and solar components of
11 hemispheric ^{14}C , *Geophysical research letters*, 25, 329-332, 1998.

12 Suthhof, A., Ittekkot, V., and Gaye-Haake, B.: Millennial-scale oscillation of
13 denitrification intensity in the Arabian Sea during the late Quaternary and its potential
14 influence on atmospheric N_2O and global climate, *Global Biogeochemical Cycles*, 15,
15 637-649, 2001.

16 Thunell, R. C., Sigman, D. M., Muller-Karger, F., Astor, Y., and Varela, R.: Nitrogen
17 isotope dynamics of the Cariaco Basin, Venezuela, *Global Biogeochemical Cycles*, 18,
18 doi:10.1029/2003GB002185, 2004.

19 You, Y.: Intermediate water circulation and ventilation of the Indian Ocean derived
20 from water-mass contributions, *Journal of marine research*, 56, 1029-1067, 1998.

21 Zonneveld, K., Versteegh, G., Kasten, S., Eglinton, T. I., Emeis, K. C., Huguet, C.,
22 Koch, B., de Lange, G. J., De Leeuw, J., and Middelburg, J. J.: Selective preservation
23 of organic matter in marine environments; processes and impact on the sedimentary
24 record, *Biogeosciences*, 7, 483-511, 2010.

1 Table 1. AMS ^{14}C dates of sediment core SK177/11. Radiocarbon ages were
 2 calibrated using CALIB 6.0 program (<http://calib.qub.ac.uk/calib/calib.html>, Reimer
 3 *et al.*, 2009).

Lab code	Depth cm	Dating materials	pMC	Raw ^{14}C age (yr BP)	Calibrated age (yr BP) (1 σ)	$\delta^{13}\text{C}$ (‰)
KIA24386	58	OM	65.58 \pm 0.17	3390 \pm 20	3186 \pm 24	-18.55 \pm 0.04
KIA26327	125	OM	46.65 \pm 0.20	6125 \pm 35	6504 \pm 26	-20.02 \pm 0.10
KIA24387	155	OM	31.38 \pm 0.13	9310 \pm 30	10054 \pm 104	-19.50 \pm 0.08
KIA26328	175	OM	21.96 \pm 0.12	12180 \pm 45	13618 \pm 104	-17.71 \pm 0.18
KIA24388	205	OM	13.94 \pm 0.11	15830 \pm 60	18646 \pm 54	-21.65 \pm 0.15
KIA24389	275	OM	9.81 \pm 0.12	18650 \pm 100(-90)	21774 \pm 194	-18.02 \pm 0.10
KIA26329	355	OM	2.76 \pm 0.06	28830 \pm 180	32857 \pm 207	-19.23 \pm 0.17

4 OM-Organic matter; pMC-Percent modern

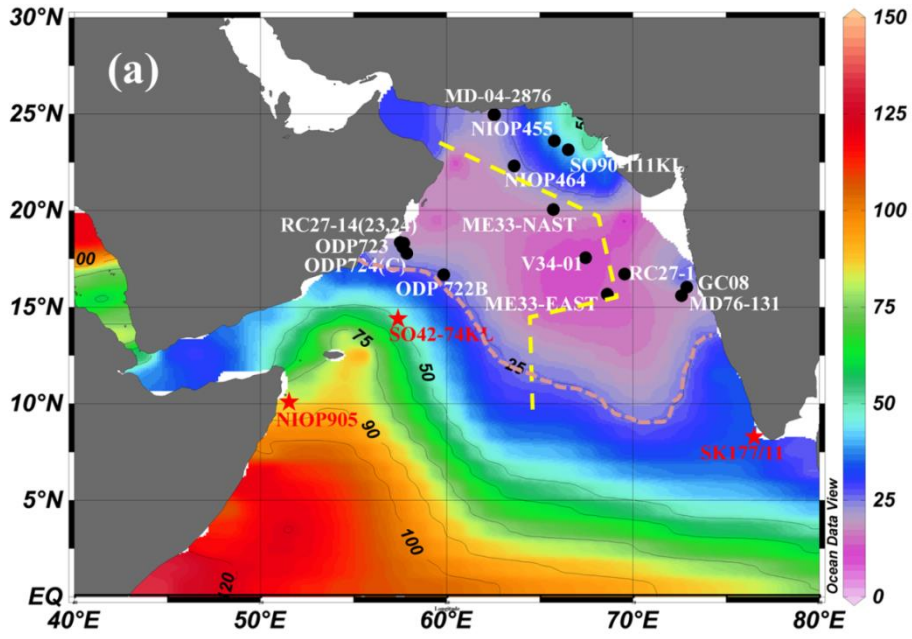
5

1 Table 2. Linear equations of bottom-depth effect during different climate stages

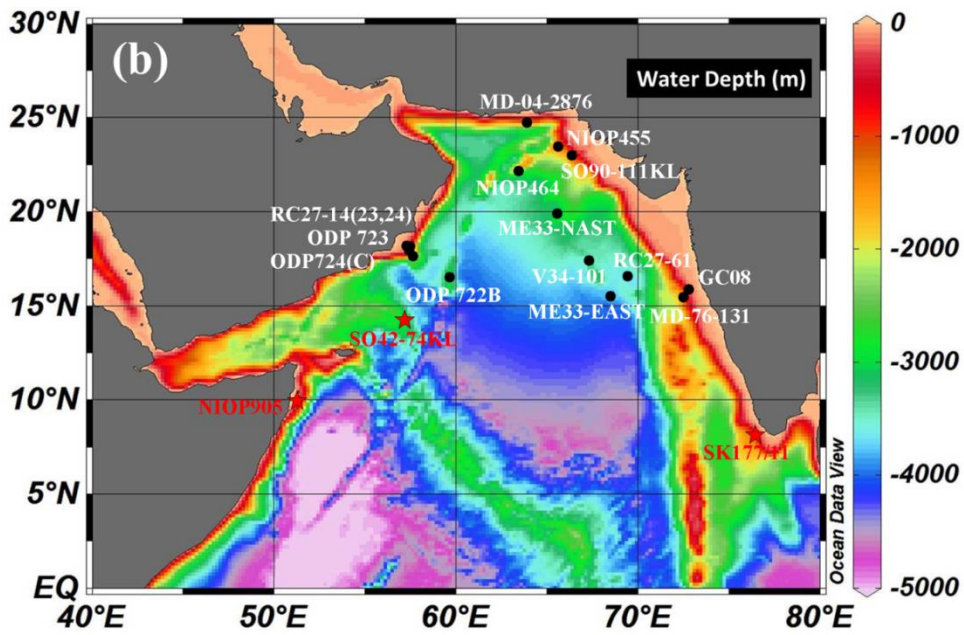
Location	Northern AS	Southern AS
Modern	$\delta^{15}\text{N} = 0.55 (\pm 0.08) \times 10^{-3} \times$ Depth + 8.1 (± 0.2) ($R^2 = 0.40$, n = 78, P < 0.0001)	$\delta^{15}\text{N} = 0.76 (\pm 0.14) \times 10^{-3} \times$ Depth + 6.0 (± 0.3) ($R^2 = 0.66$, n = 18, P < 0.0001)
Holocene	$\delta^{15}\text{N} = 0.70 (\pm 0.20) \times 10^{-3} \times$ Depth + 6.7 (± 0.3) ($R^2 = 0.61$, n = 16, P = 0.0067)	$\delta^{15}\text{N} = 0.93 (\pm 0.06) \times 10^{-3} \times$ Depth + 5.7 (± 0.1) ($R^2 = 1.00$, n = 3, P = 0.0152)
Glacial	$\delta^{15}\text{N} = 0.64 (\pm 0.20) \times 10^{-3} \times$ Depth + 5.2 (± 0.3) ($R^2 = 0.68$, n = 16, P = 0.0013)	$\delta^{15}\text{N} = 1.01 (\pm 0.31) \times 10^{-3} \times$ Depth + 4.3 (± 0.7) ($R^2 = 0.91$, n = 3, *P = 0.1899)

2 *insignificant by P value

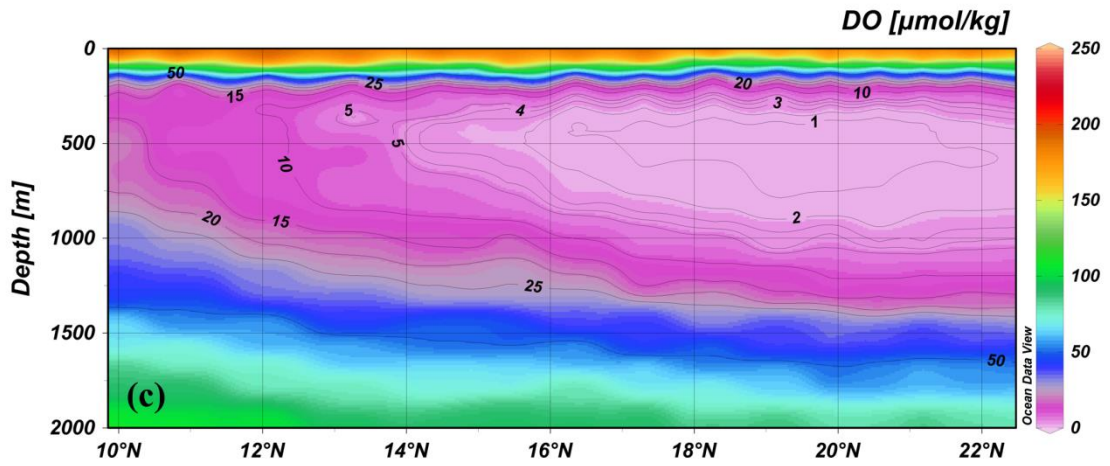
3



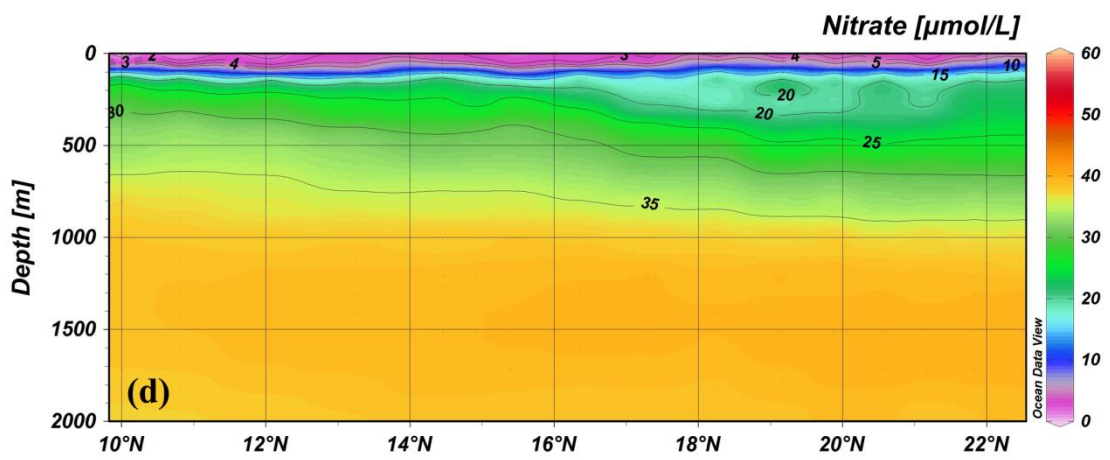
1



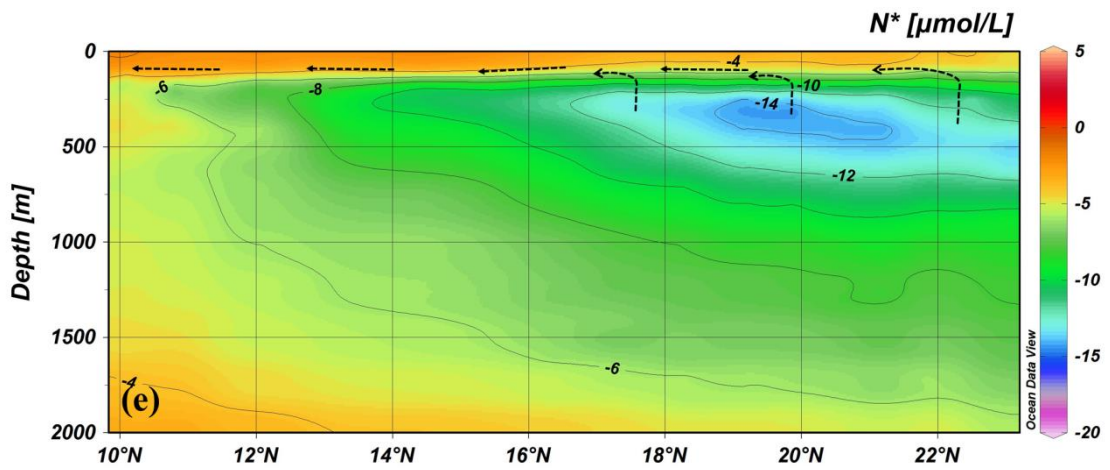
2



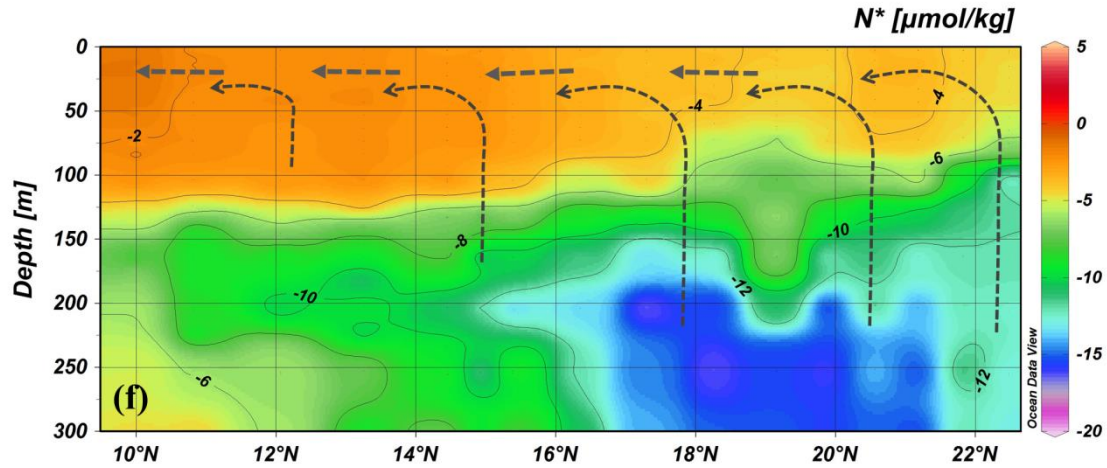
1



2



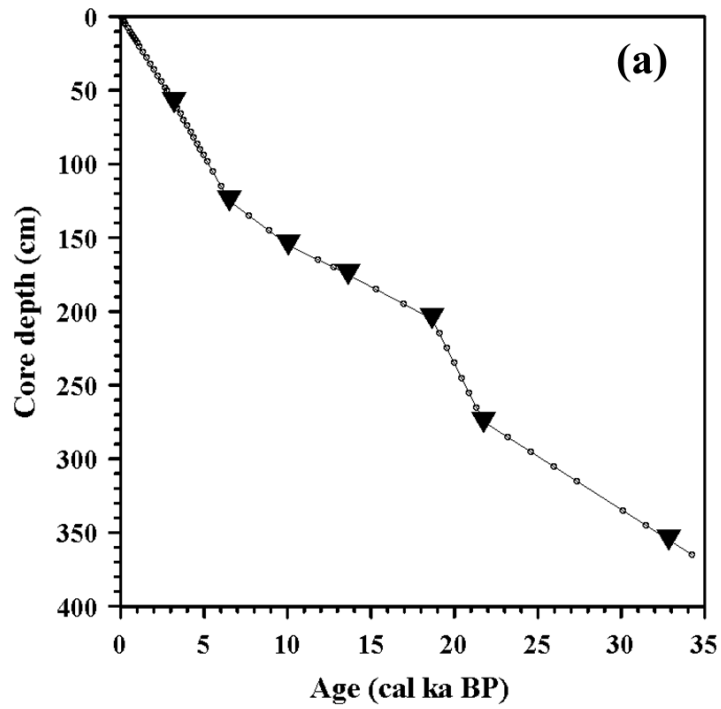
3



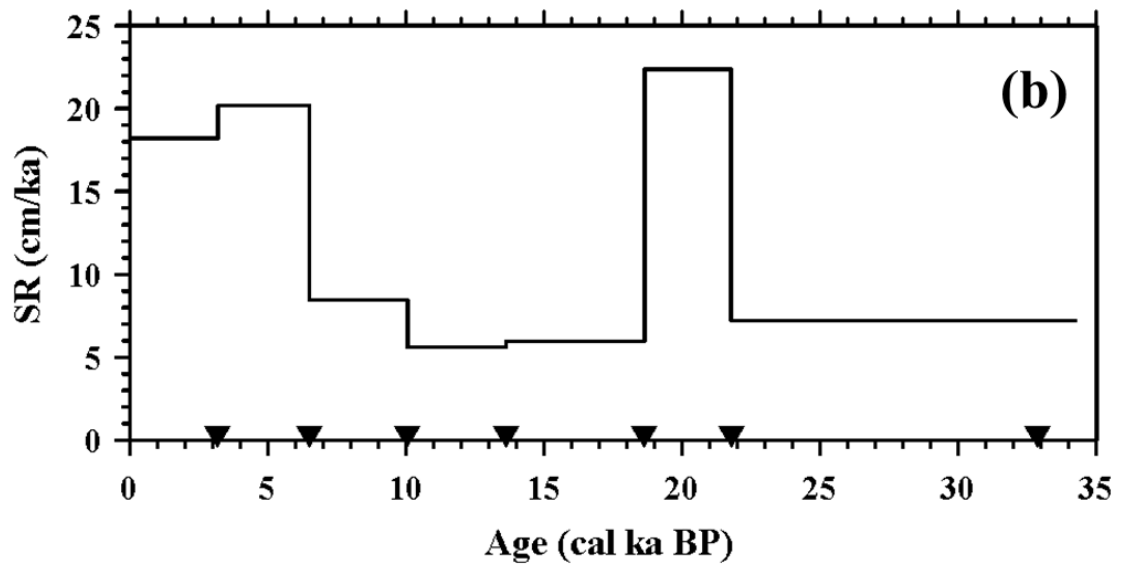
1

2

3 Figure 1. (a) Map of the Arabian Sea. Dissolved oxygen (DO) concentration at 150 m
 4 (World Ocean Atlas 09) was shown in color contour. Southern (★) and northern (●)
 5 categories of available cores and SK177/11 in this study were defined by DO of 25
 6 $\mu\text{mol kg}^{-1}$ (see text, purple dash curve). (b) Bathymetric map superimposed by core
 7 locations; (c), (d) and (e) are DO, nitrate and N^* transects (yellow dashed line in (a),
 8 online data originated from cruises of JGOFS in 1995), respectively, for upper 2000 m.
 9 (f) N^* transect for the upper 300m with arrows revealing the flow direction. In (a), the
 10 northern cores include core MD-04-2876 (828 m, Pichevin et al., 2007), core
 11 NIOP455 vs. NIOP464 (1002 m vs. 1470 m, Reichart et al., 1998), SO90-111KL vs.
 12 ME33-NAST(775 m vs. 3170 m, Suthhof et al., 2001), ODP724C vs. ME33-EAST
 13 (603 m vs. 3820 m, Möbius et al., 2011), RC27-24 vs. RC27-61 (1416 m vs. 1893 m,
 14 Altabet et al., 1995), ODP723, ODP722(B) vs. V34-101 (808 m, 2028 m vs. 3038m,
 15 Altabet et al., 1999), RC27-14 vs. RC27-23 (596 m vs. 820 m, Altabet et al., 2002),
 16 GC08 (2500 m, Banakar et al., 2005), MD-76-131 (1230 m, Ganeshram et al., 2000);
 17 the Southern cores include core SO42-74KL (3212 m, Suthhof et al., 2001), NIOP905
 18 (1586 m, Ivanochko et al., 2005) and SK177/11 (776 m, this study).



1

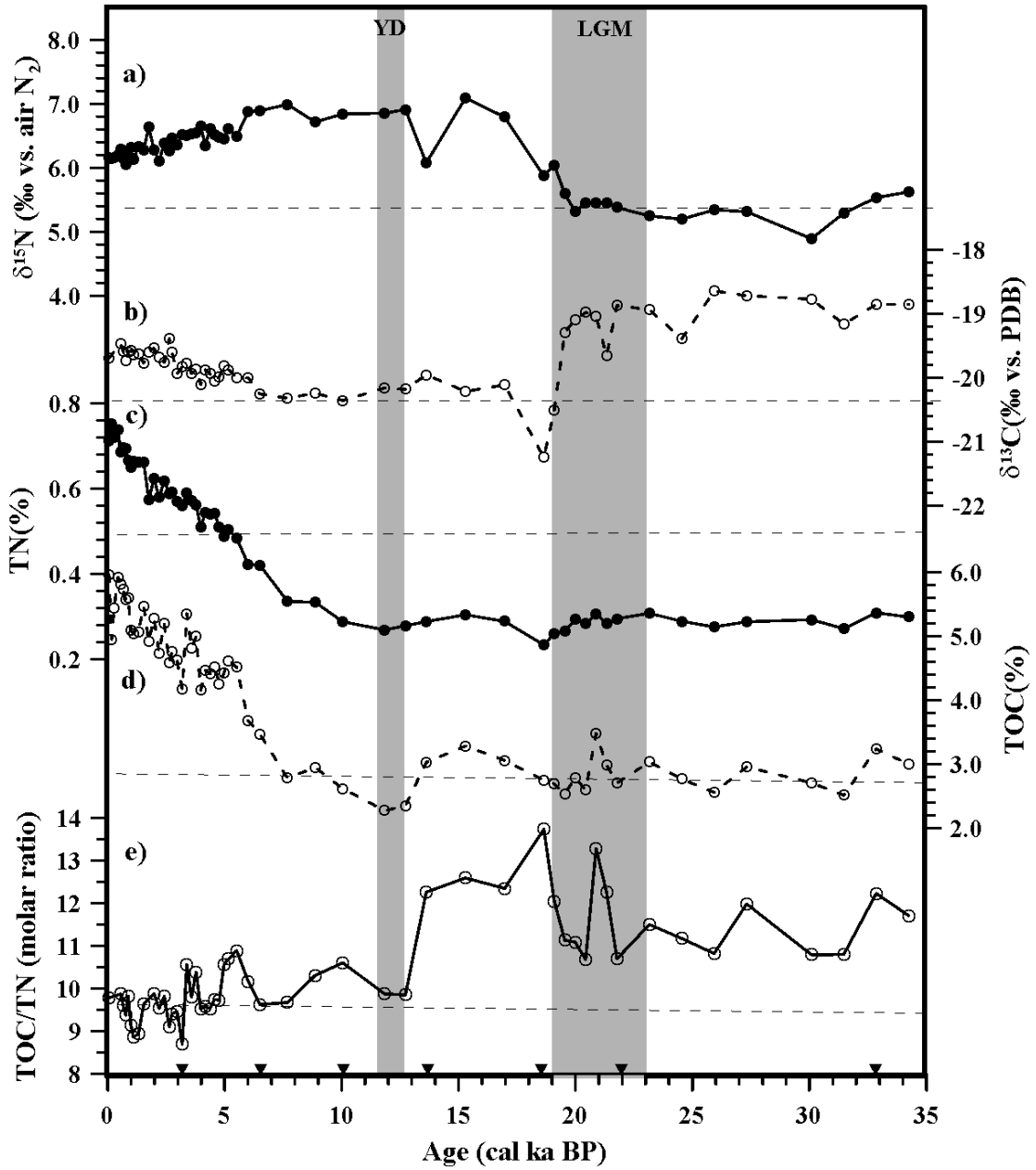


2

3

4 Figure 2. (a) Plot of calendar age against depth; (b) Linear sedimentation rate (▼
5 indicates the ^{14}C age controlling points).

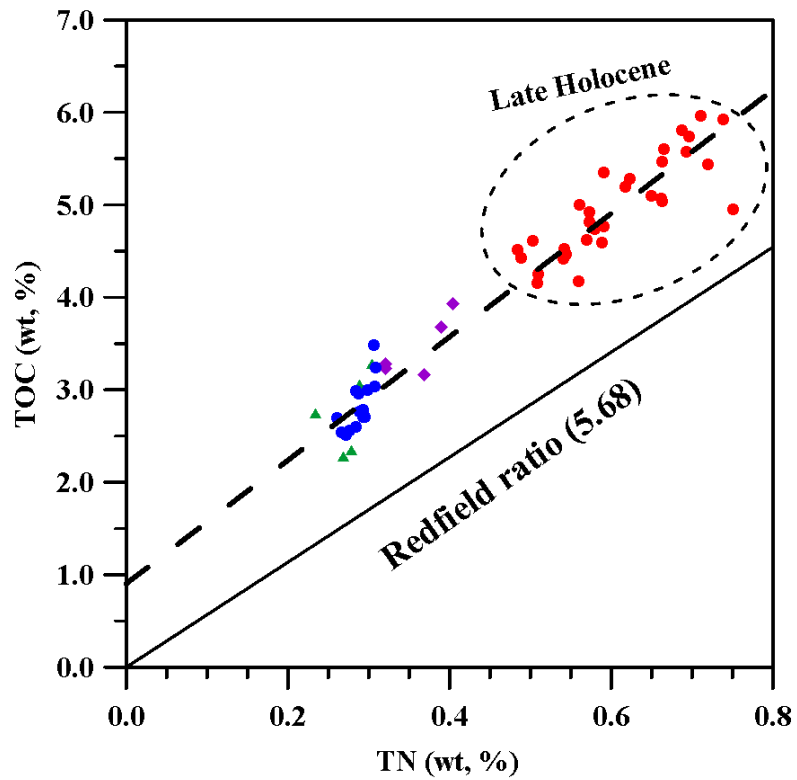
1



2

3

4 Figure 3. Temporal variations of (a) stable isotopic compositions of bulk nitrogen
5 ($\delta^{15}\text{N}$), (b) stable isotopic compositions of TOC ($\delta^{13}\text{C}$), (c) contents of total nitrogen,
6 (d) total organic carbon and (e) TOC/TN ratio.. Horizontal dashed lines are references
7 for low value periods.



1

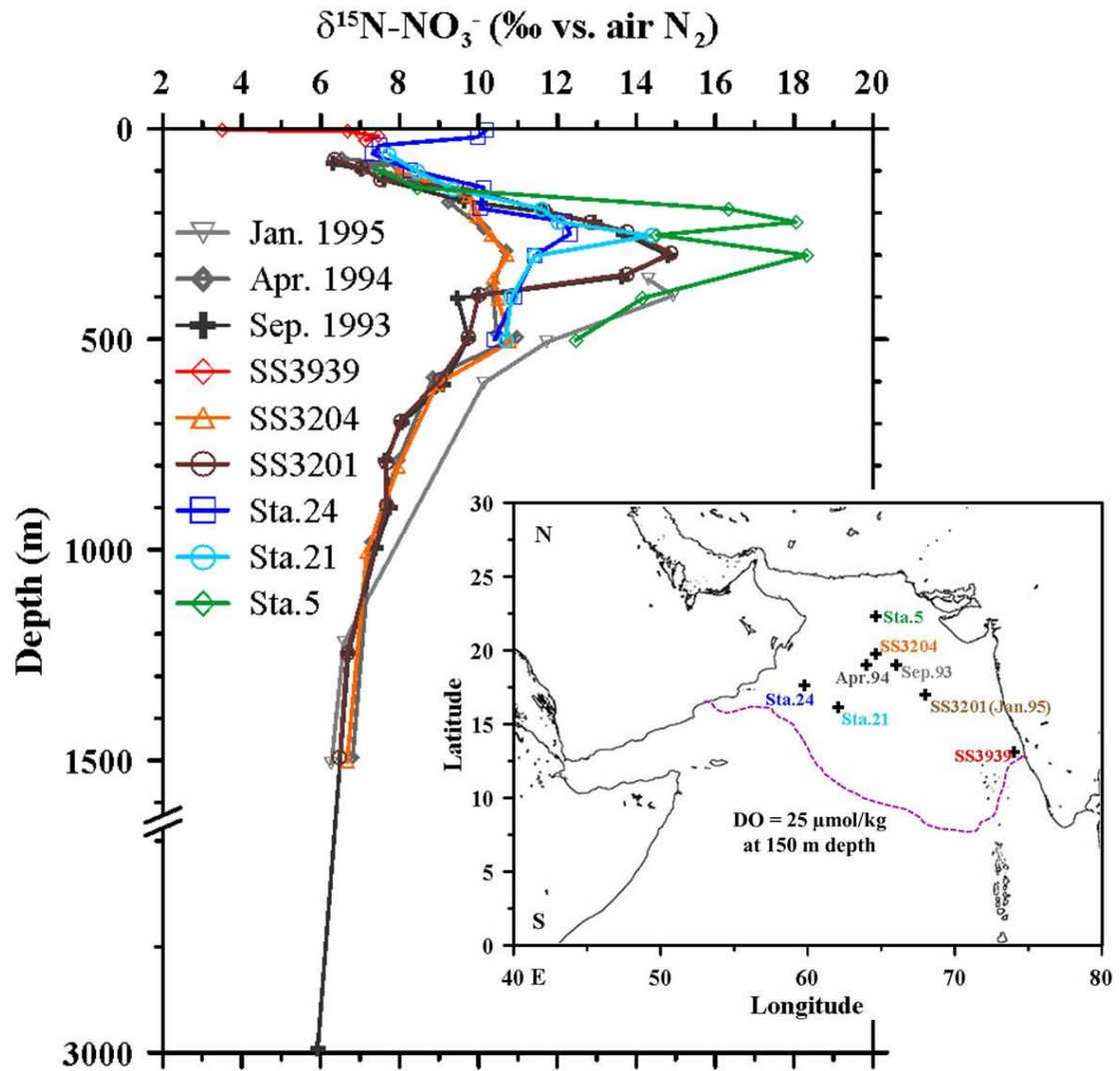
2

3 Figure 4. Scatter plot of the total organic carbon content against total nitrogen.

4 Redfield field ratio of 5.68 is shown in line. Bold dashed line stands for regression.

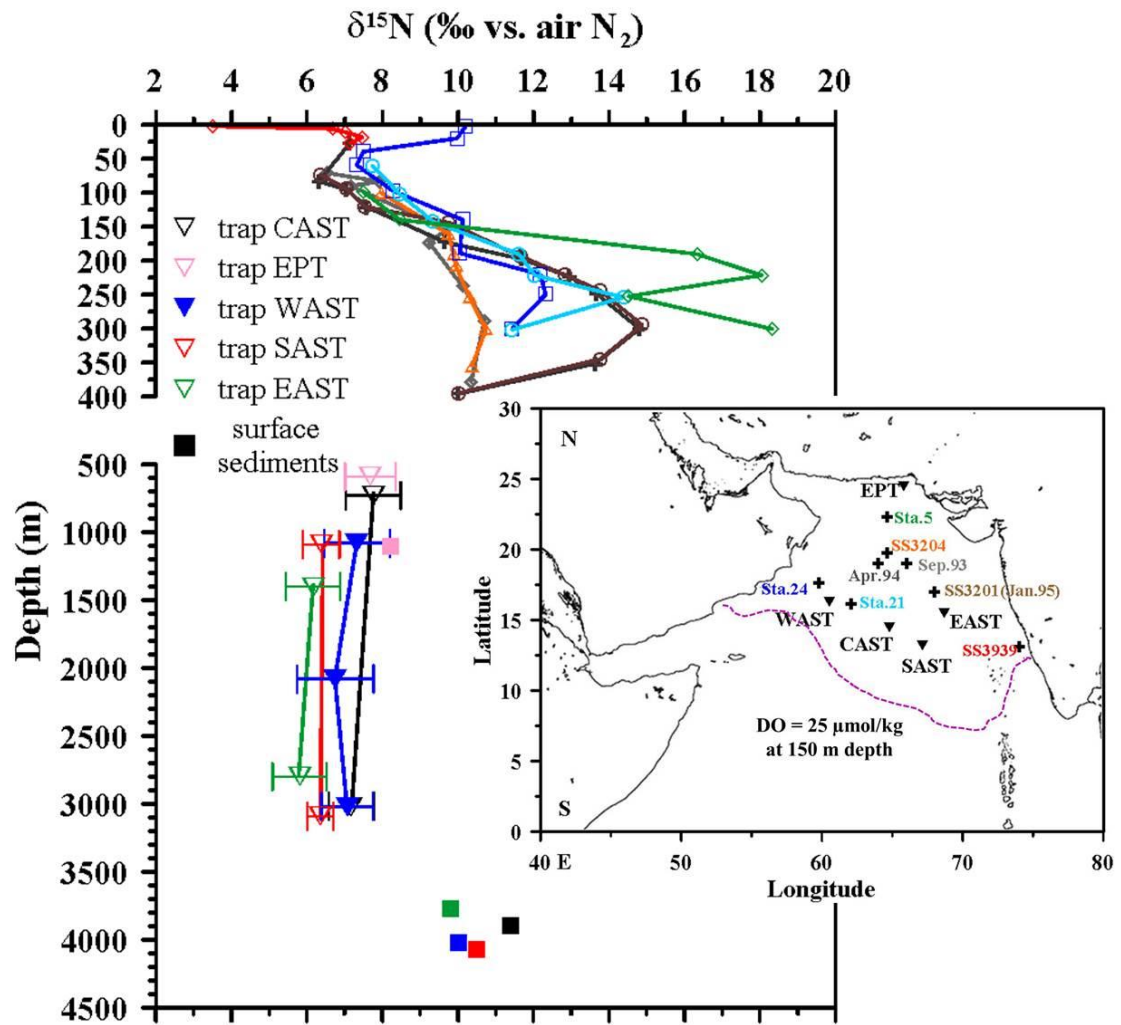
5 Red, purple, green and blue dots represent the late Holocene, early Holocene,

6 deglacial and glacial periods, respectively.



1
2

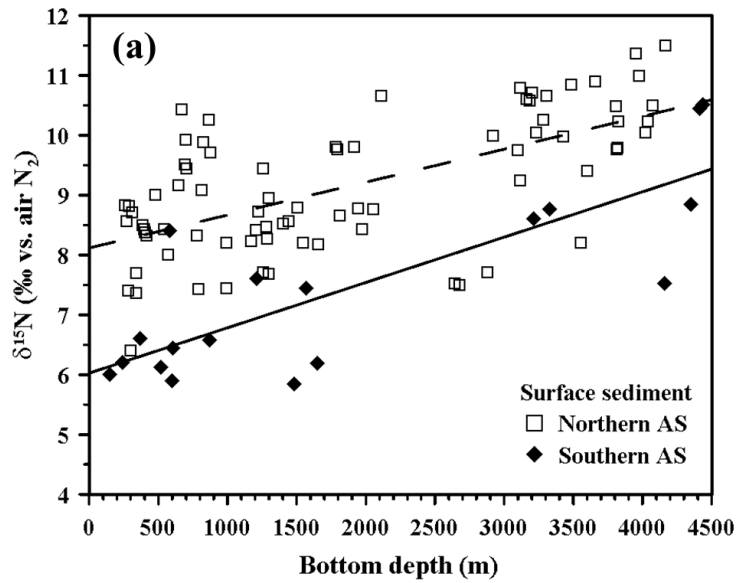
3 Figure 5. Depth profiles of nitrogen isotope of nitrate ($\delta^{15}\text{N}_{\text{NO}_3}$) in water column (data
4 without months in mark are all from August and Sta. Jan. 1995 overlaps with Sta.
5 SS3201) (Data digitized from Brandes et al., 1998; Altabet et al., 1999; Naqvi et al.,
6 2006).



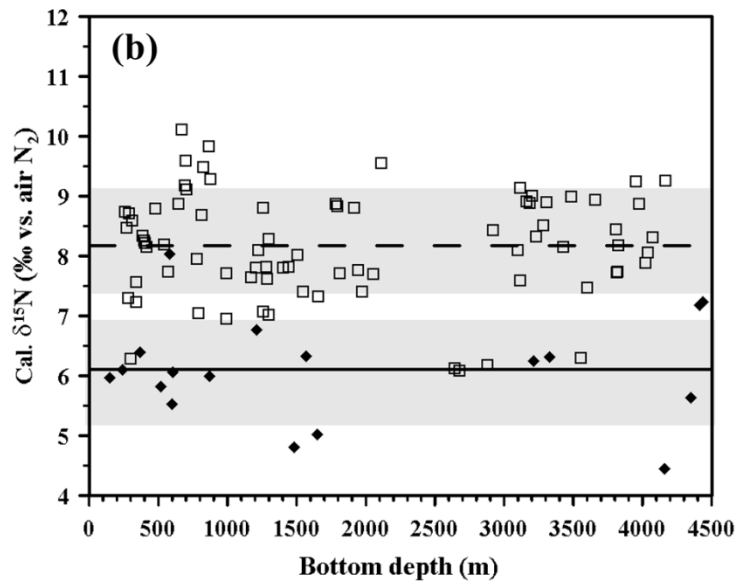
1

2

3 Figure 6. Vertical profiles for nitrogen isotope of nitrate (crosses in inserted map),
 4 sinking particles (inverse triangles in map) and trap-corresponding surface sediments.
 5 Data for sediment traps and surface sediments are from Gaye-Haake et al. (2005).
 6 Depth profile of $\delta^{15}\text{N}_{\text{NO}_3}$ follows that in Figure 5.



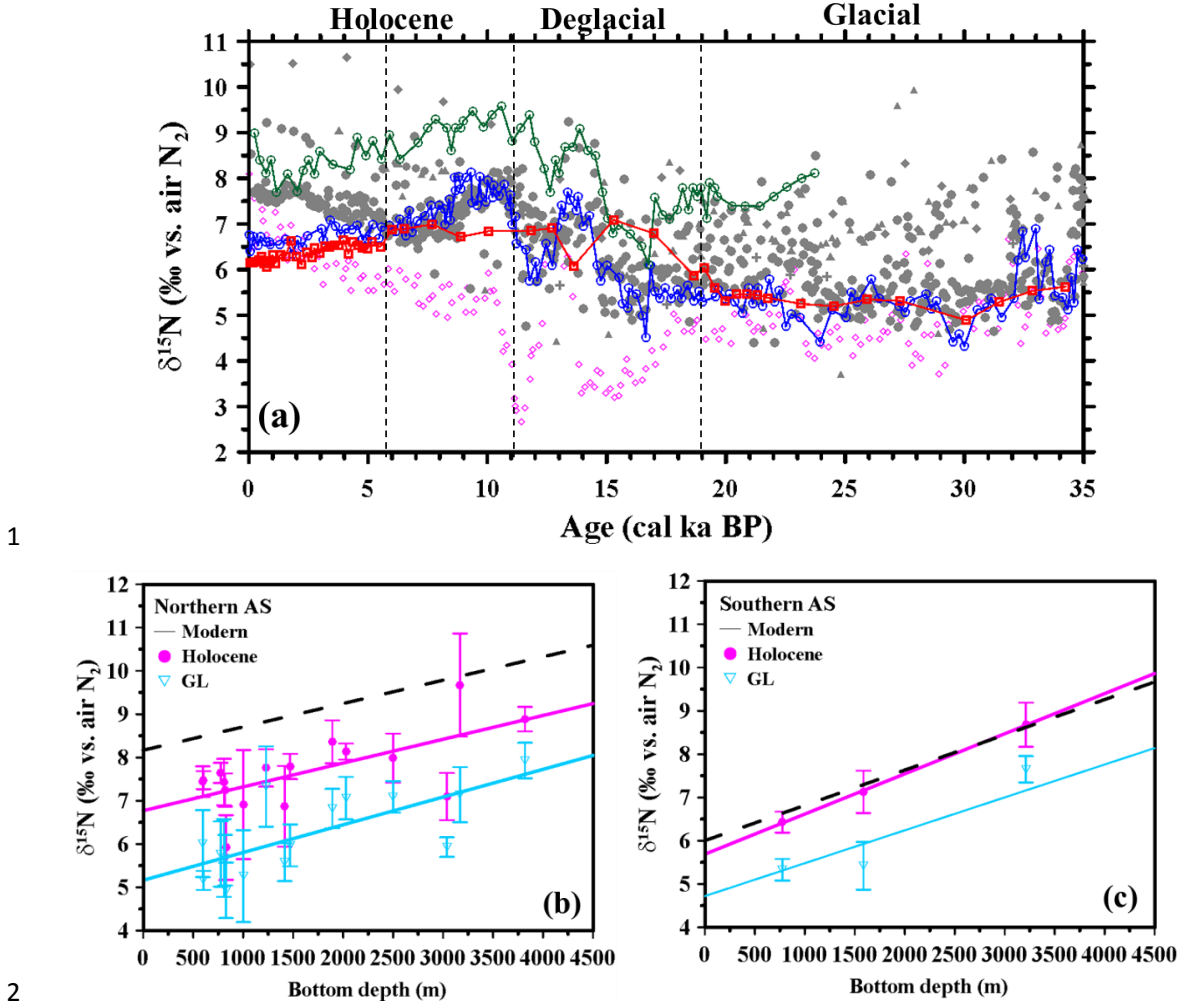
1



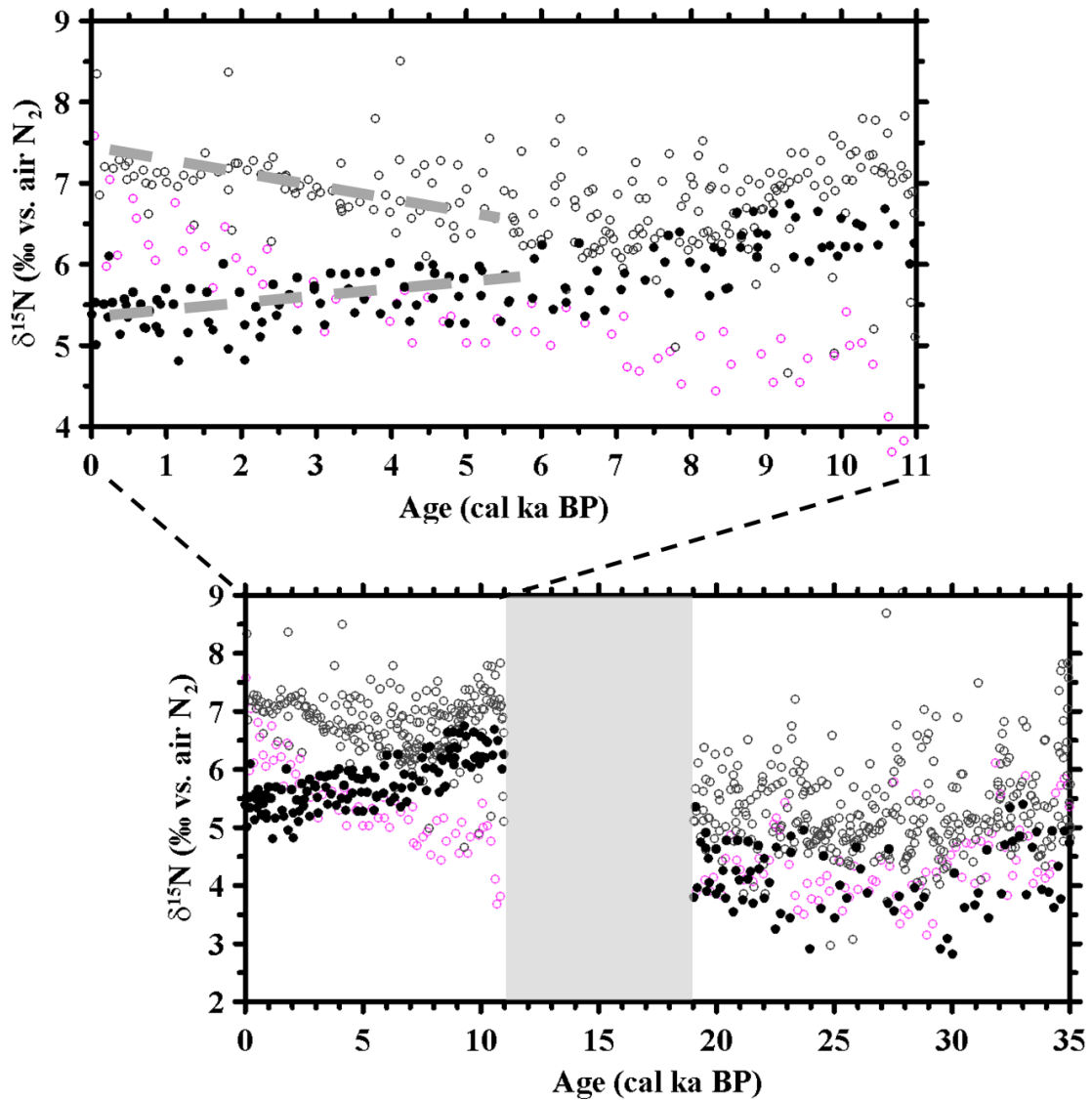
2

3

4 Figure 7. (a) Non-corrected $\delta^{15}\text{N}$ values of modern surface sediments against
 5 corresponding bottom depth in northern and southern Arabian Sea (see text for N-S
 6 boundary). Regression lines were shown in dashed and solid lines, respectively, for
 7 northern and southern AS. (b) Corrected surface sedimentary $\delta^{15}\text{N}$ values against
 8 water depth.



1
 2
 3
 4 Figure 8. (a) Temporal variations of non-corrected $\delta^{15}\text{N}_{\text{bulk}}$ values of all reported cores
 5 in the AS. Data shown in curves are for cores in the southern Arabian Sea (red for
 6 SK177/11, blue for NIOP 905 and green for SO42-74KL), dots in grey are for the
 7 northern part (pink dots are for core MD-04-2876). Mean values of $\delta^{15}\text{N}$ for fixed
 8 periods against corresponding water depths for cores in (b) northern and (c) southern
 9 Arabian Sea. Pink and indigo blue are for Holocene and glacial periods, respectively.
 10 Error bars represent the standard deviation for mean $\delta^{15}\text{N}_{\text{bulk}}$. The dashed regression
 11 lines for modern surface sediments are shown for reference.



1
2

3 Figure 9. Temporal variations of corrected $\delta^{15}\text{N}_{\text{bulk}}$ values of all reported cores in the
 4 AS. Gray and black dots are for northern and southern AS, respectively. Pink dots are
 5 specifically for core MD-04-2876. The deglacial period is in shadow because non
 6 proper equations for bottom-depth effect correction. The upper panel is the blow-up
 7 for the Holocene period. The intensified deviation trends since 6 ka were marked by
 8 bold dashed lines.